Title

Pseudomonas **taxonomic and functional microdiversity in the wheat rhizosphere is cultivar-dependent and links to disease resistance profile and root diameter**

Authors

Courtney Horn Herms[1], Rosanna Catherine Hennessy[1], Frederik Bak[1,2], Ying Guan[1], Patrick Denis Browne [1], Tue Kjærgaard Nielsen [1], Lars Hestbjerg Hansen [1], Dorte Bodin Dresbøll[3], Mette Haubjerg Nicolaisen[1]

[1]Section for Microbial Ecology and Biotechnology, [3]Section for Crop Sciences, Department of Plant and Environmental Sciences, University of Copenhagen, Thorvaldsensvej 40, Frederiksberg C, 1871 Denmark

[2]Bioresources Unit, AIT Austrian Institute of Technology, Konrad-Lorenz-Straße 24, 3430, Tulln, Austria

Abstract

The rhizosphere microbiome contributes to crop health in the face of disease pressures. Increased diversity and production of antimicrobial metabolites are characteristics of the microbiome that underpin microbial-mediated pathogen resistance. A goal of sustainable agriculture is to unravel the mechanisms by which crops assemble beneficial microbiomes, but precise understanding of the ability of the plant to manipulate intragenus microdiversity is unclear. Through an integrative approach combining culture-dependent methods and long-read amplicon sequencing, we demonstrate cultivar-dependent taxonomic and functional microdiversity of the rhizocompetent and bioactive *Pseudomonas* genus associated with *Fusarium*-resistant versus susceptible winter wheat cultivars. The resistant cultivar demonstrated increased *Pseudomonas* taxonomic but not biosynthetic diversity when compared to the susceptible cultivar, correlating with a thinner root diameter of the resistant cultivar. We found enrichment of antifungal *Pseudomonas* isolates, genes (chitinase), and biosynthetic gene clusters (pyoverdine) in the resistant cultivar. Overall, we highlight cultivar-dependent microdiversity of *Pseudomonas* taxonomy and functional potential in the rhizosphere, which may link to root morphology and play a role in crop susceptibility to disease.

Introduction

Plants and soil microorganisms interact through such a tight collaboration that the plant and its associated microorganisms are considered a holobiont (Mesny et al., 2023). A vital function of the rhizosphere microbiome for the future of agriculture is increased crop resistance to phytopathogens. However, it remains unclear how crops recruit disease-suppressive microbes to their roots, and understanding this phenomenon is a goal for enhancing microbiome-mediated disease resistance in

the field. To increase microbe-mediated disease suppression in crops we must first understand the mechanisms that drive the recruitment of specific microbes to plant roots.

The rhizosphere microbiome generally assembles into a stable community comprised primarily of the phyla Actinobacteria, Bacteroidetes, Firmicutes, and Proteobacteria, which harbor key functions important for plant health such as triggering induced systemic resistance and antagonism of pathogens (Bai et al., 2022). Current methods to understand the role of the plant microbiota in disease suppression evaluate differences between susceptible and resistant cultivars in their recruitment of antifungal phyla or genera (K. Yang et al., 2023) or overall microbiome diversity (Berg et al., 2017). Diversity within lower taxonomic levels, i.e., microdiversity (Moore et al., 1998), also plays a role in the suppression of phytopathogen invasion through resource and niche competition as well as direct antagonism (Hu et al., 2016; Jousset et al., 2011; Li et al., 2023; T. Yang et al., 2017). Since genes involved in competition and direct antagonism are often part of lineage-specific gene pools (Shalev et al., 2021), a thorough understanding of the role of microdiversity in disease suppression is needed.

Despite this, only a few studies to date have attempted to explore intragenus diversity of rhizosphere microbiomes (Mauchline et al., 2015; Oni et al., 2019; Pacheco-Moreno et al., 2021; Sondo et al., 2023). The lack of a finer taxonomic resolution in many microbiome studies of the plant holobiont may be a consequence of short-read amplicon-based analyses that conceal taxonomic diversity and functional differences between closely related microbes (Chiniquy et al., 2021; Edgar, 2018; N. R. Wang et al., 2022). Advances in sequencing technologies are increasingly lengthening amplicons, allowing for better culture-independent identification of microbes (Stevens et al., 2023), but isolation efforts and whole genome sequencing remain the gold standard for the identification of intragenus microdiversity (Huang et al., 2023).

A genus of particular interest for the study and manipulation of microdiversity for plant health is *Pseudomonas*, thanks to its intrinsic intragenus genomic diversity (Girard et al., 2021; Loper et al., 2012; Lopes et al., 2018) and assortment of secondary metabolites (Gavriilidou et al., 2022; Gross & Loper, 2009; S. Gu et al., 2020). The *Pseudomonas* genus produces a wide spectrum of proven antifungal molecules such as siderophores, phenazines, cyclic lipopeptides (CLPs), and chitinases (Mauchline & Malone, 2017; Pacheco-Moreno et al., 2021), making them a key member of disease-resistant microbiomes (Hong et al., 2023; Lv et al., 2023; Qiu et al., 2022). In the field, *Pseudomonas* can represent between 0.32% to 1.69% of the rhizosphere microbiome (Mauchline et al., 2015; Simonin et al., 2020). Despite their low abundance, *Pseudomonas* remain pervasive in the soil environment due to their highly adaptive traits (Durán et al., 2021; Getzke et al., 2023).

A key plant trait contributing to microbial community diversity is root exudation (Feng et al., 2023; Sasse et al., 2018; K. Yang et al., 2023), but it alone cannot fully explain rhizosphere microbiome assembly (Takamatsu et al., 2023). Other factors have been examined with varying levels of success. Using knockouts, single plant genes have been shown responsible for modulating plant-associated *Pseudomonas* communities (S. Song et al., 2023; Y. Song et al., 2021). Irrigation, on the other hand, failed to explain the distribution of suppressive *Pseudomonas* isolates in potato fields (Pacheco-Moreno et al., 2021). Additional hypotheses for the role of the physical landscape including root morphology have been suggested as additional mechanisms driving community diversity (Dubey et al., 2021; Herms et al., 2022). The physical and chemical landscapes implicated by different root phenotypes have the potential to modulate root-microbe interactions (Herms et al., 2022).

Specifically, there is growing evidence for a link between thinner root diameter and bacterial diversity in the rhizosphere for both woody and herbaceous species (Fleishman et al., 2023; King et al., 2023; Luo et al., 2021; Pervaiz et al., 2020; Saleem et al., 2018; Zai et al., 2021). However, to date no studies correlating intragenus microdiversity to root diameter exist.

In the present work, we explored the root-associated *Pseudomonas* taxonomic and functional microdiversity of two commercially available cultivars of winter wheat (*Triticum aestivum L.*) grown in agricultural soil. Two cultivars with different field resistance to the wheat pathogen *Fusarium columorum* were selected: the moderately resistant Sheriff cultivar and the moderately to highly susceptible Heerup cultivar (Jørgensen et al., 2020, 2023). To examine the microdiversity of the wheat-associated *Pseudomonas* community, we undertook an integrative approach combining culture-dependent and culture-independent analyses, coupled to root scanning that determined root morphology differences between the cultivars. We hypothesized that taxonomic and functional microdiversity is driven by crop cultivar. Specifically, we hypothesized that the *Fusarium*-resistant cultivar, Sheriff, harbors a more diverse *Pseudomonas* community due to the contribution of microbial diversity to plant resistance to pathogens. In relation to this, we hypothesized that the Sheriff cultivar has a thinner average root diameter than the Heerup cultivar due to the link between root diameter and microbiome diversity. Lastly, we hypothesized that the Sheriff cultivar hosts more antifungal activity, genes linked to antifungal activity, and biosynthetic gene clusters (BGCs) for antifungal secondary metabolites, which may contribute to the demonstrated field resistance against *F. culmorum*.

Materials and Methods

Wheat cultivation and sampling

Two winter wheat (*Triticum aestivum* L.) cultivars, Heerup and Sheriff, were chosen based on their documented resistance to Fusarium Head Blight (FHB) in the field and were supplied by Sejet Plant Breeding (Horsens, Denmark). One seed of each cultivar was sown in a 24 x 7 cm PVC pot filled with soil mixed with sand (DANSAND, Denmark; filter sand no. 2) in a 2:1 ratio. The soil was a sandy loam collected from the plough layer (0-25 cm) in the University of Copenhagen's Long Term Nutrient Depletion Experiment located at Højbakkegård in Høje Taastrup, Denmark (van der Bom et al., 2018). The soil had received mineral NPK fertilizer at a rate of 120 kg nitrogen, 20 kg phosphorus and 120 kg potassium $ha^{-1}y^{-1}$ for the past 25 years and contained 170 g kg^{-1} clay, 174 g kg^{-1} silt, 336 g kg^{-1} fine sand, 255 g kg^{-1} coarse sand, and 40 g kg^{-1} organic matter. The soil had a pH($CaCl_2$) of 5.4, an Olsen-P content of 11.4, and the water holding capacity (WHC) was 33%. The soil was air-dried and sieved to 8mm prior to the experiment.

The plants were grown under controlled greenhouse conditions in three stages: an 18-day germination period (19°C day/15°C night; 16h day/8h night; light intensity 300 µE), followed by a 13-week vernalization period (6°C day/4°C night; 8h day/16h night; light intensity 150 µE), and finally a 17-week growth period to maturity (19°C day/15°C night; 16h day/8h night; light intensity 500 µE). Pots were regularly rotated and watered to 70% WHC by weighing.

Three different time points were sampled (Methods Fig. 1). After four weeks, plants were sampled for root morphology scanning. Plants were sampled at first node emergence (T1) for *Pseudomonas* isolation and a first round of long-read 16S rRNA amplicon sequencing, and at flag leaf emergence (T2) for a second round of long-read 16S rRNA amplicon sequencing.

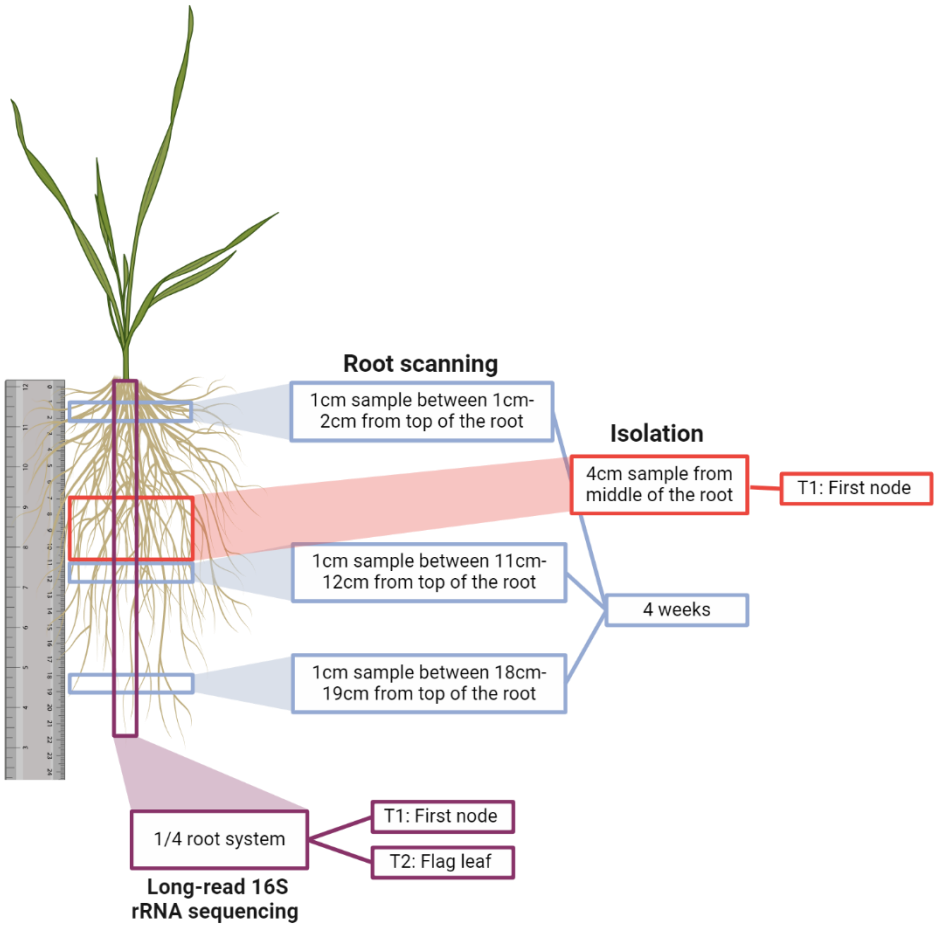

Methods Figure 1. Sampling for Pseudomonas isolation, long-read 16S rRNA amplicon sequencing, and root scanning occurred along different root axis as well as across different time points. Created with Biorender.com.

Pseudomonas library building

Three replicate plants were sampled at first node emergence (T1) to obtain *Pseudomonas* colonies (Methods Fig. 1). To obtain rhizoplane samples, one gram (corresponding to approximately 4 cm) of root was washed in 25 mL sterile PBST (10% 10x PBS, 0.1% Tween 80) and subsequently placed in 25 mL of fresh, sterile PBST. The roots were sonicated in a water bath for two minutes to release rhizoplane soil and microorganisms. To isolate *Pseudomonas* species, 50 µL of undiluted and a 1:10 dilution in PBST (10% 10x PBS, 0.1% Tween 80) of the rhizoplane sample was plated onto Gould's S1 media (Gould et al., 1985) to select for *Pseudomonas* isolates. After incubation at room temperature for two to four days, single colonies were streaked for purification first on Gould's S1 media and a second time on Luria-Bertani (LB) agar (Miller, 1972). Isolates were maintained as frozen stocks (15% glycerol w/w).

16S rRNA gene sequencing of cultured isolates

A modified version of colony PCR (von Stein et al., 1997) was used to amplify the full-length 16S rRNA gene of the isolates in the strain library. A 30 µL PCR reaction mixture was prepared: 15 µL Master Mix (Supreme NZYTaq II 2x Master Mix, NZYTech, Portugal), 0.6 µL of 10 µM forward and reverse primer (27F, 1492R; Weisburg et al., 1991), 11.8 µL Sigma water, and 2 µL 1:1000 diluted overnight culture. The cycling conditions were as follows: preliminary boiling step of 96°C for 5 min

144 followed by 25 cycles of denaturing at 98°C for 10 s, annealing at 57°C for 30 s, extension at 72°C for
145 45 s, and a final extension of 10 min at 72°C. Successful amplification of the 16S rRNA gene was
146 visualized on 1% agarose gels. PCR purification and Sanger sequencing of the PCR product was
147 completed by Eurofins (Germany). The ends of the reads were trimmed based on quality scores.
148 Reads of short length (<900 base pairs (bp)) were manually discarded using CLC Genomics
149 Workbench (v. 12.0.03) (QIAGEN).

150 Sequences were oriented to the same strand using USEARCH (Edgar, 2010) and the RDP training set
151 (v. 18) as reference and then aligned using MUSCLE (Edgar, 2004). Gaps at the end of the aligned
152 sequences were removed using Gblocks (Castresana, 2000). Sequences were clustered into
153 sequence variant cluster of 100% identity using the USEARCH *cluster_fast* command (Edgar, 2010).
154 The 16S rRNA sequences from each sequence variant cluster were submitted to NBCI BLASTn for
155 alignment to the 16S rRNA database (Altschul et al., 1997).

156 The 16S rRNA genes of the strain library isolates are available in Genbank under accession numbers
157 PP894319-PP894691.

158 ### Phenotypic assays

159 The wheat fungal pathogen *Fusarium culmorum* was sporulated in Mung bean media (Ilmi et al.,
160 2019) (20 grams boiled mung beans, strained, in 1 L distilled water). A high-throughput, agar-based
161 confrontation assay was developed to screen the strain library for antifungal activity. Briefly, the
162 *Pseudomonas* isolates were inoculated onto a pre-germinated lawn of 1.45 x 10^3 *F. culmorum* spores
163 on 1/5 potato dextrose agar (BD DIFCO, Denmark). After three days of co-inoculation at room
164 temperature, the isolates were scored for their ability or inability to inhibit *F. culmorum* growth. A
165 positive result required a clearance zone of at least 1 mm around a colony. *Serratia inhibens* S40
166 (Hennessy et al., 2020) was used as the positive control.

167 A high throughput drop collapse assay (Bodour & Miller-Maier, 1998) was used to screen the strain
168 library for biosurfactant production. The isolates were grown in 1.5 mL liquid LB media for four days
169 in a deep-well 96-well plate at 28°C while shaking (200 rpm). To test for biosurfactant production, 40
170 µL of culture was pipetted onto Parafilm, and at least two minutes passed before the droplet size was
171 measured. Water was used as the negative control, and *P. fluorescens* SBW25, which produces the
172 surfactant viscosin (Alsohim et al., 2014), was used as the positive control.

173 ### Genome sequencing and bioinformatics pipeline

174 All unique culture sequence variant (CSV) clusters identified from the strain library via 16S rRNA
175 gene sequencing were subject to full genome sequencing. CSV clusters containing many isolates
176 were sequenced deeper, proportional to the size of the CSV cluster and how many isolates in the
177 CSV cluster originated from each cultivar. Genomic DNA was prepared from overnight cultures using
178 the QIAGEN Genomic DNA Handbook using the QIAGEN Buffer Kit (Germany) or the Genomic Mini
179 Ax Bacteria 96-Well kit (A&A Biotechnology, Poland) according to the manufacturer's instructions.
180 Quality was checked using a NanoDrop ND-1000 spectrophotometer (Thermo Fisher Scientific,
181 Carlsbad, CA, USA) prior to library building. Genomic DNA was prepared for sequencing using the
182 Rapid Barcoding Sequencing Kit (SQK-RBK004) or the Rapid Sequencing gDNA barcoding kit (SQK-
183 RBK110.96) and sequenced on MinION and PromethION flow cells (v. 9.4.1) (Oxford Nanopore
184 Technologies, United Kingdom). Reads were basecalled with Guppy (v. 6.2.1) using the "super
185 accuracy" dna_r9.4.1_450bps_sup.cfg basecalling model. Adapter sequence and barcodes were

186 trimmed from basecalled reads with Porechop (v. 0.2.4). Genomes were assembled using Flye (v.
187 2.9-b1774) (Lin et al., 2016; Kolmogorov et al., 2019), polished with Medaka (v. 1.7.1)
188 (https://nanoporetech.github.io/medaka), and annotated using Prokka (v. 1.14.6) (Seemann, 2014)
189 using default parameters. The quality of the genomes was assessed using CheckM (v1.1.10) (Parks et
190 al., 2015). Genomes not passing thresholds for completeness (> 90.0%) and contamination (< 2.0%)
191 were removed from future analyses. Dereplication with dRep (v. 3.4.5) (Olm et al., 2017) and the
192 Genome Taxonomy Database Toolkit (v. 2.3.0) (Chaumeil et al., 2020; Parks et al., 2020) were used
193 to delineate and identify species and strains. In dRep, 95% average nucleotide identity (ANI) was
194 chosen to delineate species, and 99.55% ANI was used to delineate strains.

195 The annotated genomes were screened for secondary metabolite prediction with antiSMASH (v. 7.0)
196 (Medema et al., 2011) using the standard cutoff of 0.3, *glocal* mode, and the *include_singletons* flag.
197 BiG-SCAPE (v. 1.1.7) (Navarro-Muñoz et al., 2020) and the MiBIG database (v. 3.1) (Terlouw et al.,
198 2023) were used for biosynthetic gene cluster family analysis. Anvi'o (v. 7.0) (Eren et al., 2021) was
199 used to assign functions using NCBI's Clusters of Orthologus Groups (COGs) database (Tatusov et al.,
200 2000), generate a pangenome, and quantify functional enrichment between sets of genomes
201 (Shaiber et al., 2020). A phylogenetic tree was generated from single-copy core genes using trimAl
202 (Capella-Gutiérrez et al., 2009) and the 'WAG' general matrix model from IQ-TREE (Minh et al., 2020)
203 to infer a maximum likelihood tree.

204 The fully assembled genomes are available under BioProject accession number PRJNA1108081.

205 Long-read 16S rRNA gene amplicon sequencing

206 For long-read 16S rRNA amplicon sequencing, rhizoplane samples were obtained as described above
207 at first node (T1) and flag leaf (T2) emergence (Methods Fig. 1). After the sonication step, the
208 rhizoplane samples were flash frozen in liquid nitrogen and freeze-dried. DNA was extracted using
209 the FastPrep-24 5G bead-beating system (MP Biomedicals, Irvine, CA, USA) at 6.0 m/s for 40 s and
210 the FastDNA SPIN Kit for soil (MP Biomedicals) according to the manufacturer's instructions.

211 PCR reactions were prepared with 32.5 µL Sigma water, 10 µL SuperFi Buffer (Thermo Fischer), 0.5
212 µL Platinum SuperFi DNA Polymerase (Thermo Fischer), 1 µL 10 mM dNTPs, 2.5 µL each of 10 nM
213 forward and reverse primer (TAG Copenhagen, Denmark), and 1 µL DNA template diluted to 5 ng/µL.
214 *Pseudomonas*-specific primers for amplifying 969 bp of the 16S rRNA gene (position 289-1258) were
215 used (forward primer 5'-GGTCTGAGAGGATGATCAGT-3' and reverse primer 5'-
216 TTAGCTCCACCTCGCGGC-3') (Widmer et al., 1998). ZymoBIOMICS Microbial Community DNA was
217 used as a sequencing control (Zymo Research, Irvine, CA, USA). The cycling conditions were as
218 follows: preliminary denaturation step of 98°C for 30 s followed by 30 cycles of denaturing at 98°C
219 for 10 s, annealing at 63°C for 30 s, extension at 72°C for 45 s, and a final extension of 10 min at
220 72°C. Successful amplification was visualized on 1% agarose gels. PCR products were purified using
221 AMPure XP beads at a 0.6 ratio (Beckman Coulter Inc. Brea, CA, USA). Amplicons were prepared for
222 sequencing using a native barcoding kit (Oxford Nanopore SQK-NBK114.96) and sequenced on a
223 Minion (Oxford Nanopore) on an R10.4.1 flow cell (Oxford Nanopore FLO-MIN114). Raw nanopore
224 data was basecalled with Guppy (v. 6.3.9) using the "super accuracy" basecalling model
225 dna_r10.4.1_e8.2_260bps_sup-v4.1.0.

226 Adapters were trimmed from Nanopore reads using porechop (v. 0.2.4)
227 (https://github.com/rrwick/Porechop) with the following options: adapter_threshold 95,

228 extra_end_trim 0, end_threshold 95, middle_threshold 95, extra_middle_trim_good_side 0,
229 extra_middle_trim_bad_side 0, min_split_read_size 800. The options were used to filter out overly
230 short inserts and to leave the primer sequences in the trimmed reads. Following this, primer
231 sequences were identified, and the intervening sequences (inserts) were extracted using
232 strip_degen_primer_deep (github.com/padbr/asat) and inserts between 880 and 970 nt were
233 retained. High quality inserts (Phred quality ≥ 30) were identified using Nanofilt (De Coster et al.,
234 2018). High quality inserts were then dereplicated and unique sequences counted using the
235 fastx_uniques utility of usearch (v. 11.0.667) (Edgar, 2010), and zero-width amplicon sequencing
236 variants (ASVs) were inferred using unoise3 (Edgar, 2016). All read inserts trimmed of adapters and
237 primers, within the 880 to 970 nt range, but not quality filtered, were used to create a ASV table
238 using the otutab utility of usearch.

239 The raw reads are available under BioProject accession number PRJNA1108081.

240 ## Root morphology scanning

241 To measure root morphology of the two cultivars, 4-week old plants were removed from the pots
242 and all soil was rinsed from the roots using tap water. Samples of 1 cm length were taken 1 cm (top),
243 11 cm (middle), and 18 cm (bottom) from the top of each root (Methods Fig. 1). Images of each
244 section of root were photo-scanned using the Epson Perfection V700 scanner (8-bit gray scale, 600
245 dpi), and root diameter was measured using RhizoVision (v. 2.0.3) using "broken roots" analysis
246 mode (Seethepalli et al., 2021). To remove debris and artifacts from the analysis, a maximum object
247 size was set at 10 mm^2, and edge smoothing was set at a threshold of three. After segmentation,
248 root pruning was performed with a threshold of 50. Root diameter ranged were manually set at 0-
249 0.2 mm, 0.2-0.3 mm, 0.3-0.4 mm, 0.4-0.5 mm, 0.5-1.0 mm, and 1.0-1.5 mm. After RhizoVision
250 analysis, the percentage of the root system in each of diameter class of the three root sections were
251 averaged to obtain a single percentage for each plant replicate.

252 ## Statistical analysis

253 All statistics were performed in R (v. 4.3.1). The rarefaction plot was generated using vegan (v. 2.6-4)
254 (Oksanen et al., 2022). Calculating the effect of cultivar on antifungal activity, biosurfactant
255 production, and unique isolates was performed by Fischer's Exact test. When comparing means, all
256 data were tested for normality using the Shapiro-Wilk test. The two-sided Wilcoxon Rank Sum test
257 was used in place of a two-sided unpaired Student T test when normality could not be assumed. P
258 values were adjusted for multiple testing as appropriate using the Benjamini & Hochberg method
259 (Benjamini & Hochberg, 1995). An analysis of variance model (ANOVA) was fitted to compare
260 percentages of the root system within each root diameter class and to assess the effects and
261 interaction between cultivar and diameter class. A separate ANOVA was also fitted using an
262 interaction variable between cultivar and diameter class. Plots were made using ggplot2 (v. 3.4.2).

263 Long-read amplicon sequencing data were analyzed using Qiime2 (Caporaso et al., 2010).
264 Normalization of the ASV table was done by rarefying with all ASVs. Following this, the ASV table was
265 filtered to keep only features classified in the *Pseudomonas* genus. Qiime2 was then used to derive
266 values for α-diversity (richness, Chao1, and Shannon) and β-diversity (Bray-Curtis dissimilarity). The
267 Shannon diversity values were converted to effective Shannon diversity by raising two to the power
268 of the Shannon diversity (the Shannon diversity was calculated using two as the logarithmic base, as
269 Qiime2 uses scikit-bio (https://zenodo.org/records/8209901)). Composition data and α-diversity

metrics were compared between groups of samples using the Mann-Whitney U-test to test for significance. ASVs were omitted from composition tests if the ASV is not seen in at least 50% of the samples in one of the groups. Anosim (Clarke, 1993), with 999 permutations, was used to test if two or more groups of samples differed from each other.

Results

1) Culture-based screening indicates a more diverse and antifungal Sheriff *Pseudomonas* microbiome

A strain library of 373 pseudomonads comprising 195 isolates from Heerup and 178 isolates from Sheriff was successfully isolated and taxonomically profiled using full-length 16S rRNA gene sequencing. Clustering at 100% identity across a minimum of 900 bp and an average of 1114 bp of the 16S rRNA gene resulted in 65 unique culture sequence variant (CSV) clusters, and BLASTn alignment to the NBCI 16S rRNA gene database revealed 17 potential *Pseudomonas* species (Table 2). The most abundant species in the library was identified as *P. kilonensis* with 143 isolates, followed by *P. extremaustralis* and *P. baetica* with 86 and 36 isolates, respectively. Initial observations suggested preference of certain taxa to one cultivar over the other, with Sheriff demonstrating a tendency to harbor more uniquely recruited pseudomonads (Figure 1). Seven and three species and 36 and 17 CSVs were uniquely recruited to the Sheriff and Heerup cultivar, respectively. Additionally, the Sheriff cultivar harbored more CSVs than the Heerup cultivar; 33 CSVs were found in Heerup and 59 in Sheriff (Figure 1B) (Fisher's exact test, $p = 0.0052$). However, the rarefaction curve demonstrated that the full *Pseudomonas* diversity was not sampled via isolation (Figure S1).

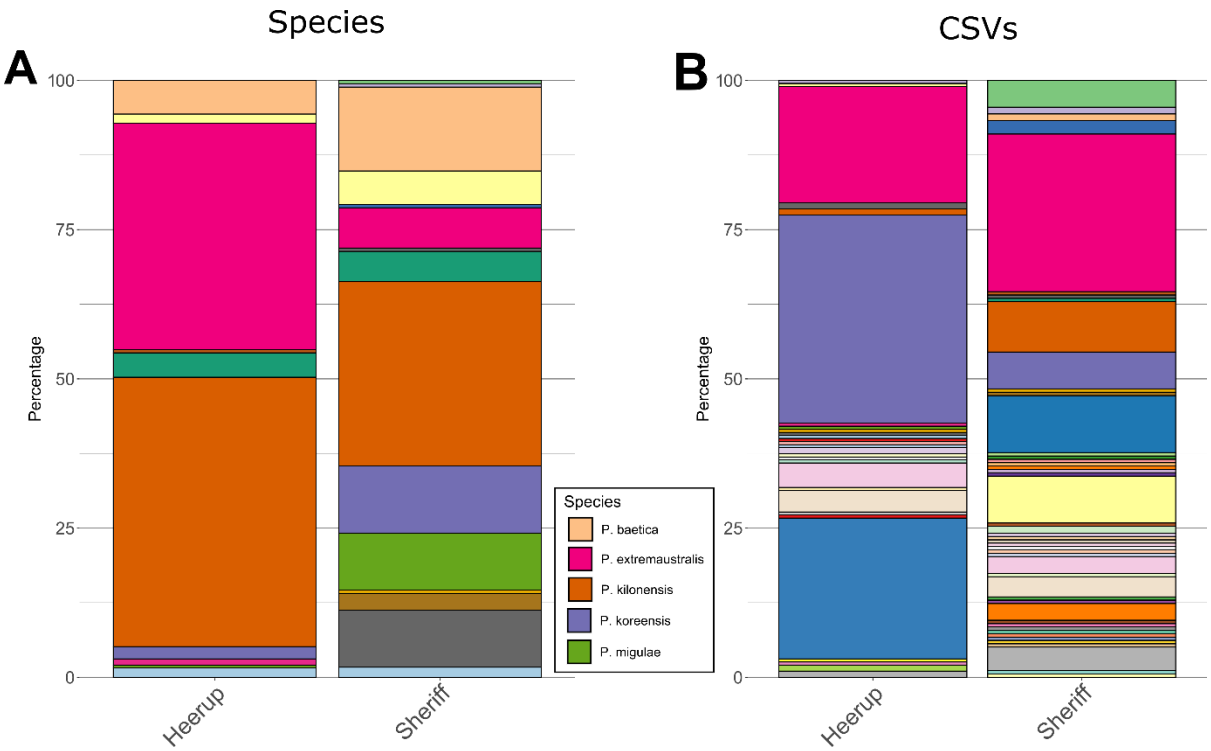

Figure 1. Composition of the Heerup and Sheriff *Pseudomonas* strain libraries identified by Sanger sequencing of minimum 900 bp of the 16S rRNA gene from 195 purified isolates from Heerup and 178 purified isolates from Sheriff. Each color represents a *Pseudomonas* species or CSV. A)

296 Composition at the species level identified by sequence alignment to the NBCI 16S rRNA gene
297 database. A legend identifying the top five most abundant species is shown. B) Composition at the
298 CSV level, defined as 100% identity across a minimum of 900 bp of the 16S rRNA gene.

299 To assess functional microdiversity within the isolated *Pseudomonas*, a high-throughput antifungal
300 screen and drop-collapse assay were performed. Across both cultivars, 33.3% (n = 129) of strains
301 inhibited growth of the fungal pathogen *F. culmorum*, whereas 17.3% (n = 67) of strains were
302 positive for biosurfactant activity. The high-throughput phenotypic screens showed that antifungal
303 isolates were enriched in the Sheriff strain library (40.0%) compared to Heerup strain library (26.6%)
304 (Fisher's exact test, $p = 0.0030$), while the proportion of biosurfactant producers did not differ
305 between Sheriff (20.5%) and Heerup (14.2%) ($p = 0.0603$) (Fig. 2).

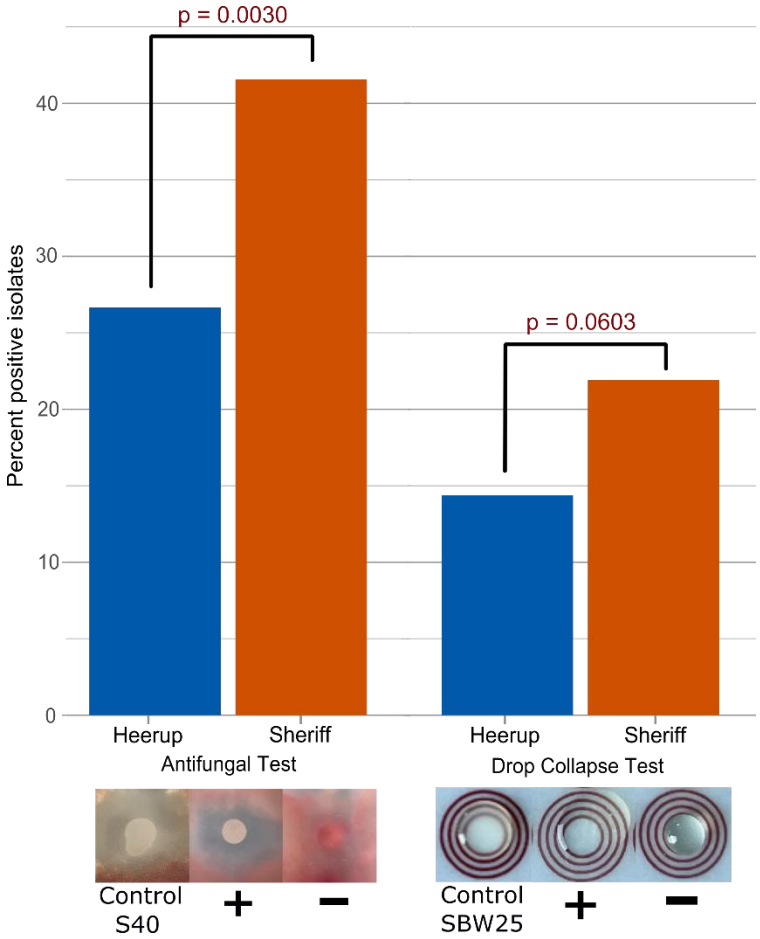

306

307 **Figure 2. The percentage of the strain libraries which can inhibit the growth of *F. culmorum in vitro***
308 **depended on cultivar of origin, but the ability to produce biosurfactants was not dependent on**
309 **cultivar. P-values of Fisher's exact test are given above the bars. Strains *Serratia inhibens* S40 and**
310 ***Pseudomonas fluorescens* SBW25 were used as the positive control for the antifungal assay and**
311 **the biosurfactant assay, respectively.**

312

313 **2) Targeted long-read 16S rRNA amplicon sequencing supports *Pseudomonas* microdiversity**
314 **and antifungal potential in Sheriff cultivar.**

315 To confirm Sheriff's enrichment of *Pseudomonas* microdiversity in a culture-independent manner,
316 long-read 16S rRNA amplicon sequencing of the rhizoplane sample was performed at the same time

317 point as the culturing (at first node emergence, T1) (Heerup and Sheriff, n = 5) and one month after
318 the culturing time point (at flag leaf emergence, T2) (Heerup n = 10, Sheriff n = 9).

319 Prior to rarefying, 373,093 reads were assigned to 707 ASVs, with a range of 2,014 to 37,612 counts
320 per sample. Seventy of the 707 ASVs were classified within the *Pseudomonas* genus. Exact matches
321 to all 16S rRNA genes pulled from the 112 genomes of the cultured, sequenced isolates (see below)
322 were found in the amplicon data, but due to the length of the amplicon at 880-970 bp, many 16S
323 rRNA gene sequences were grouped together. Twenty-two additional, uncultured *Pseudomonas*
324 ASVs were identified. However, the full *Pseudomonas* richness was still not captured with amplicon
325 sequencing (Fig S2A).

326 At T1, 67% to 91% of reads per sample were classified as *Pseudomonas* with a median of 81% (Fig
327 S2B). One uncultured pseudomonad, ASV7, dominated all samples at this time point and contributed
328 to a low percentage of cultured *Pseudomonas* reads captured by sequencing (Fig S2C). There was
329 also no significant difference in *Pseudomonas* diversity nor any ASVs differentially abundant
330 between the two cultivars at T1 (data not shown).

331 At T2, ASV7 decreased 95-fold in relative abundance. This caused a drop in *Pseudomonas* reads per
332 sample, with a range of 2% to 43% with a median of 5% (Fig S2B) and increased the percentage of
333 cultured *Pseudomonas* reads (Fig S2C).

334 At T2, Sheriff contained a higher diversity of *Pseudomonas* than Heerup (Mann-Whitney U-test, p =
335 0.00013), which aligned with the conclusion from culturing. One uncultured ASV and three ASVs
336 mapping back to five isolates were significantly enriched in the Sheriff cultivar (Table 1A). Within the
337 ASVs mapping back to cultured isolates that were enriched in the Sheriff cultivar at T2, two of the
338 isolates showed antifungal activity against *F. culmorum in vitro.*

339 Across T1 and T2, three ASVs mapping back to 12 isolates were significantly enriched in the Sheriff
340 cultivar compared to the Heerup cultivar (Table 1B). Within the ASVs mapping back to cultured
341 isolates that were enriched in the Sheriff cultivar across T1 and T2, seven of the isolates were
342 antifungal against *F. culmorum in vitro.* At no time point were there any ASVs enriched in the Heerup
343 cultivar.

344

ASV	**Antifungal isolates within ASV**	**median number of reads in Sheriff**	**median number of reads in Heerup**	**Pval**
S1E05	0/1	1.0	0.0	0.0472
S2B12_S2C03	1/2	3.0	0.0	0.0322
ASV67	n/a	1.0	0.0	0.0098
H3E07_S3A09	1/2	1.0	0.0	0.0398

345 **Table 1A. Enriched ASVs in Heerup and Sheriff at T2, with notice of the isolates that were**
346 **antifungal in the *in vitro* screen. P values were determined using the Mann-Whitney U-test. ASVs**
347 **were omitted from composition tests if the ASV is not seen in at least 50% of the samples in one of**
348 **the groups.**
349
350

ASV	Antifungal isolates within ASV	median number of reads in Sheriff	median number of reads in Heerup	Pval
H1D09_H2B05_H2D02_S1A03_S2D10_S3C01_S3E11_S3F07_S3H10	6/9	14.0	6.0	0.0305
H3E07_S3A09	1/2	1.0	0.0	0.0036
H3H08	0/1	1.0	0.0	0.0079

Table 1B. Enriched ASVs in Heerup and Sheriff across T1 and T2, with notice of the isolates that were antifungal in the *in vitro* screen. P values were determined using the Mann-Whitney U-test. ASVs were omitted from composition tests if the ASV is not seen in at least 50% of the samples in one of the groups.

3) Genome sequencing highlights *Pseudomonas* microdiversity and identifies chitinase as potential driver for enriched *Pseudomonas* antifungal activity in Sheriff cultivar

For a more detailed analysis on functional microdiversity, isolates were chosen for full-genome sequencing based on 16S rRNA gene phylogeny. Briefly, the representative isolate of each of the 65 unique CSVs was sequenced, and large CSV clusters were sequenced deeper, proportional to the size of the CSV cluster and how many isolates in the CSV cluster originated from each cultivar. A total of 112 isolates were fully genome sequenced of which 53 were isolated from Heerup and 59 were isolated from Sheriff.

Gene clusters generated based on amino acid sequence similarity were generated using Anvi'o (Eren et al., 2021). In total, 14,769 gene clusters present in at least two genomes were identified. The core genome consisted of 2,322 gene clusters. Dereplication (Olm et al., 2017) and the Genome Taxonomy Database (Chaumeil et al., 2020) identified 21 species and 48 strains in the library (Table 2). Six species and 14 strains were specific to Heerup while 10 species and 31 strains were specific to Sheriff.

	Input	Sequence used to identify taxonomy	(C/A)SVs	Species	Strains
16S Sanger sequencing	373 isolates	900- 1270 bp of 16S rRNA gene	65	17	n/a
Long-read amplicon sequencing	19 rhizoplane samples	880-970 bp of 16S rRNA gene	70	n/a	n/a
Full genome sequencing	112 isolates	Full genome	n/a	21	48

Table 2. Counts of *Pseudomonas* found during each method used in the study, based on the various taxonomic levels and their definition based on percent identity across the sequence.

373 Gene cluster analysis revealed differences in genomic content among isolates within the same
374 *Pseudomonas* species (Fig 3A). This genomic mirodiversity was, in some instances, influenced by
375 cultivar of origin. In the case of the six isolates identified as *P. brassicacearum* strain R, three loci
376 composed of 65 gene clusters, 6 gene clusters, and 9 gene clusters were present only in the four
377 isolates from the Heerup cultivar while absent in the two isolates from the Sheriff cultivar (Fig 3B). In
378 this same taxon, a locus of 24 gene clusters was present only in the Sheriff-isolated strains (Fig 3B);
379 this locus seems to be associated with the synthesis of flagella (Supplemental Table 1). Additionally,
380 there is a locus of 76 gene clusters in *P. simiae* that were only present in isolates cultured from the
381 Heerup cultivar (Fig 3C).

382 In order to link genomic microdiversity to functional potential, enrichment scores for COG20
383 pathways, categories, and functions were calculated between isolates cultured from Heerup and
384 Sheriff cultivar using Anvi'o (Eren et al., 2021). Twenty-nine COG20 categories were differentially
385 enriched between strains originating from the two cultivars (adjusted $q < 0.05$): 15 in Heerup and 14
386 in Sheriff (Supplemental Table 2). The most common differentially abundant COG20 categories
387 between the two cultivars were signal transduction mechanisms (n = 10), secondary metabolites
388 biosynthesis, transport and catabolism (n = 7), and cell membrane biogenesis (n = 7). A total of 213
389 COG20 functions were differentially enriched between strains originating from the two cultivars
390 (adjusted q-value < 0.05): 104 in Heerup and 109 in Sheriff (Supplemental Table 3). Notably,
391 chitinase family GH19 (accession: COG3179) was enriched in isolates originating from the Sheriff
392 cultivar (adjusted q-value = 9.2E-6). Of the remaining differentially enriched COG20 functions, no
393 others were known to be directly implicated in antifungal activity (Supplemental Table 2). There
394 were no differentially enriched COG20 pathways.

395

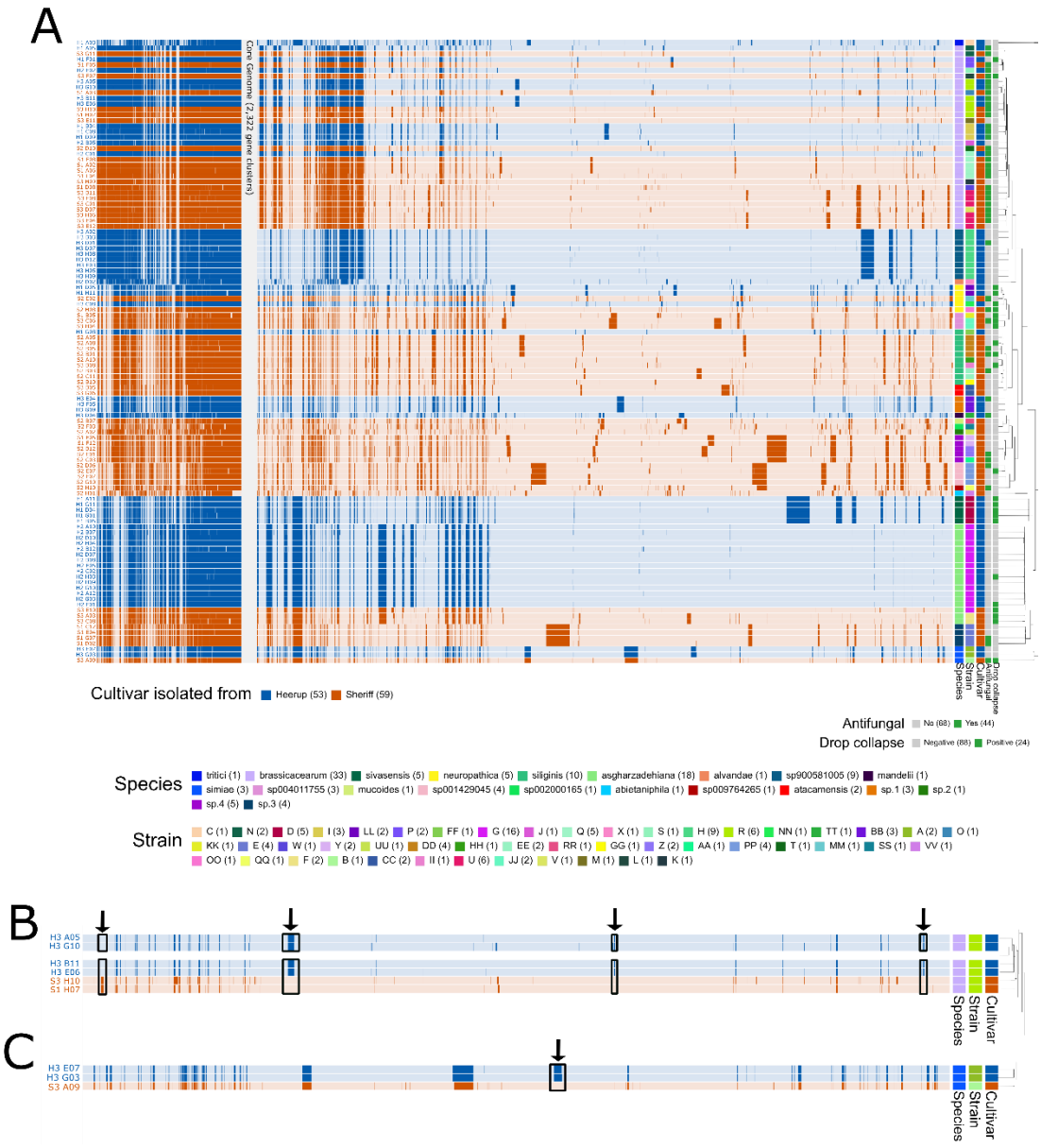

Figure 3. Pangenome of the 112 genomes. A) Blue highlight represents an isolate cultured from Heerup, and an orange highlight represents an isolate cultured from Sheriff. Shaded bars indicate the presence of gene clusters in the genome. The core genome of 2,322 gene clusters is collapsed for increased clarity. A phylogenetic tree and key metadata including species/strain identification and phenotypic assay result is indicated. B) Highlight boxes and arrows indicates the missing gene cluster locus in the Heerup-isolated strains of *P. brassicacearum* strain R, and the missing three gene cluster loci in Sheriff-isolated strains, despite its presence in closely related (same species and strain) isolates. C) Highlight box and arrow indicates the missing one gene cluster locus in Sheriff-isolated strains of *P. simiae* despite its presence in closely related (same species) isolates.

4) Genome mining reveals *Pseudomonas* functional partitioning between Heerup and Sheriff via cultivar-specific species enrichment

We mined the genomes for biosynthetic gene clusters (BGCs) to examine the biosynthetic potential of the *Pseudomonas* strain library. Screening with antiSMASH (Medema et al., 2011) and analysis via

411 BiG-SCAPE (Navarro-Muñoz et al., 2020) revealed 1315 BGCs in the strain library that grouped into
412 137 BGC families. The most common class of BGC in the strain library was ribosomally synthesized
413 and post-translationally modified peptides (RiPP, n = 450) followed by NRPS (n = 378). The most
414 common product class was RiPP-like (n = 287), followed by redox co-factors (n = 118), NRPS-like (n =
415 117), and NRPS (n = 111). The BGC families identified in the strain library were mapped to the MiBIG
416 database, and this revealed six known products (Table 3).

BGC family	**Known BGC**	**Product Class**	**Enriched in**	**Adjusted p value**
2428	3-thiaglutamate	RiPP-like	n/a	0.22
2549	Viscosin	NRPS	n/a	0.09
2653	Arthrofactin A, anikasin, lokisin, stechlisin B2	NRPS	n/a	0.84
3049	Pf-5 pyoverdine	NRPS	Sheriff	**0.0297**
3453	2,4-diacetylphloroglucinol	T3PKS	n/a	0.37
3764	Tabtoxin	blactam	n/a	0.36

417 **Table 3. BGC families in the strain library that were identified as known products and the cultivar**
418 **they were enriched in, if applicable. Significant differences in the abundance of the BGC family**
419 **between cultivars was calculated using the two-sided Wilcoxon Rank Sum test with fdr-**
420 **adjustment using the Benjamini & Hochberg method.**

421 To test the hypothesis of antifungal BGC enrichment in Sheriff, we determined BGC families that
422 were differentially abundant in Heerup and Sheriff. Overall, there were not a difference in average
423 number of BGCs in isolates from the two cultivars (two-sided Wilcoxon Rank Sum test, $p > 0.05$) (Fig
424 4A), but 28 of the 137 BGC families identified in the strain library were differentially abundant
425 between the two cultivars (two-sided Wilcoxon Rank Sum test, fdr-adjusted $p < 0.05$) (Fig 4B).
426 Nineteen and nine BGC families were enriched in Heerup and Sheriff, respectively, spanning 11
427 different product classes (Fig 4B). The only known BGC family differentially enriched between the
428 two cultivars was FAM_03049, an NRPS encoding a Pf-5 pyoverdine (Table 3). Two CLPs were
429 identified in the strain library, viscosin and lokisin, and they were not found to be different between
430 Heerup and Sheriff (Table 3).

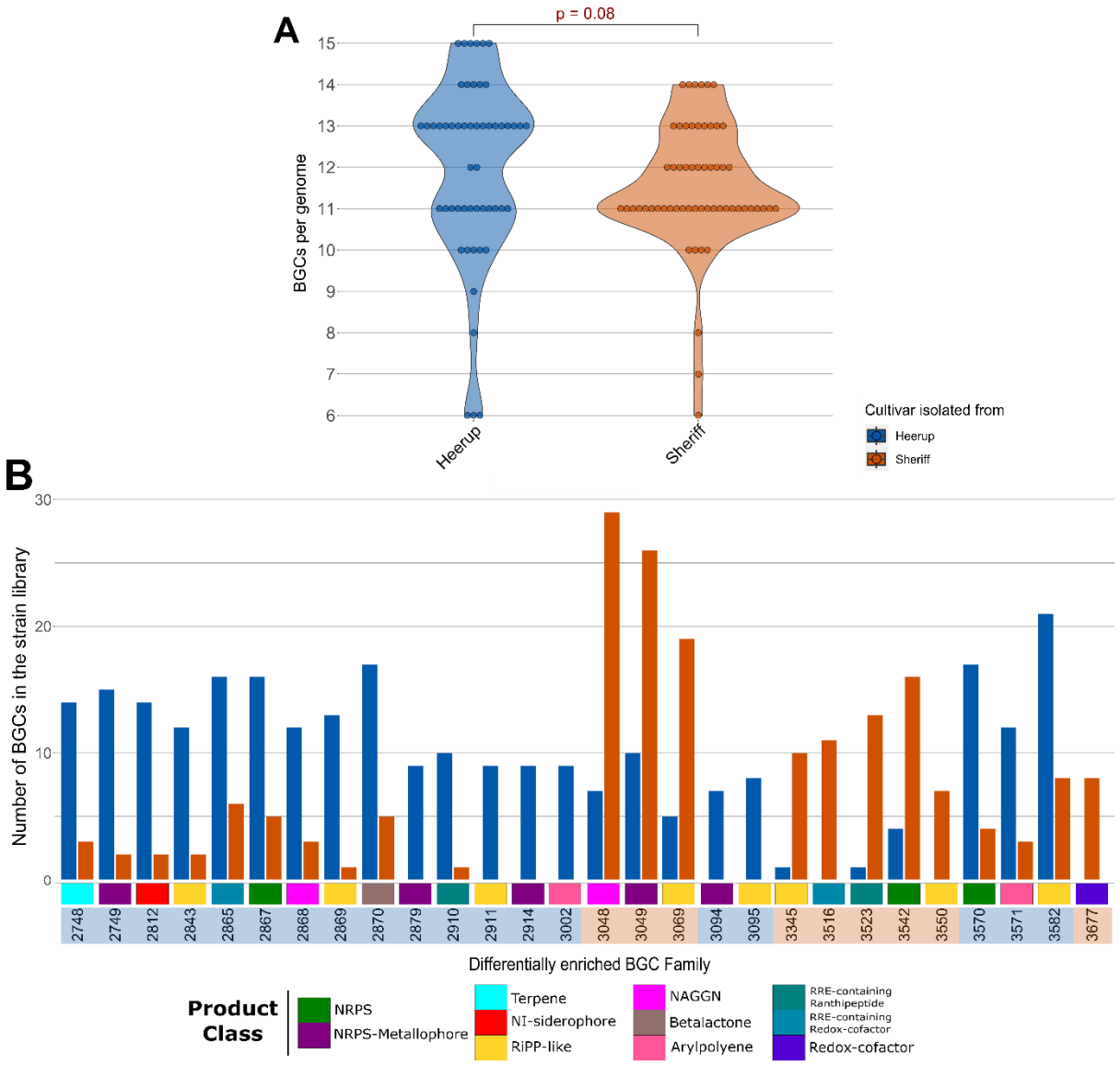

Figure 4. Differences in biosynthetic potential between the Heerup and Sheriff strain libraries. A) Number of BGCs per genome in isolates cultured from Heerup or Sheriff cultivar is not different (two-sided Wilcoxon Rank Sum test). The average number of BGCs per genome in Heerup and Sheriff is 11.98 with a standard deviation of ±2.22 and 11.53 with a standard deviation of ±1.55, respectively. B) Differentially abundant BGC families found in Heerup- or Sheriff-associated pseudomonads were calculated using the two-sided Wilcoxon Rank Sum test and multiple testing was accounted for using the Benjamini & Hochberg method. BGC families are color-coded along the x-axis by their predicted product class. X-axis highlight box indicates if the BGC family is enriched in Heerup (blue) or Sheriff (orange).

Our next objective was to uncover the factors underpinning the differing abundance of BGC families within the Heerup and Sheriff *Pseudomonas* communities. Of the three species found more than once in both cultivars, only one demonstrated cultivar-dependent average number of BGCs (Figure 5A). The average number of BGC families in the species *P. brassicacearum* was affected by cultivar (two-sided Wilcoxon Rank Sum test, $p = 0.0140$), with an average number of BGCs for Heerup and Sheriff at 11.00 ± 0.43 and 11.62 ± 0.74, respectively. However, a greater influence of species exclusivity was suggested due to the small number of species found across both cultivars. Analyzing

448 the distribution of the differentially abundant BGC families in the strain collection revealed that the
449 variation in BGC family abundance was driven by the enrichment or exclusivity of specific
450 *Pseudomonas* species harboring a given BGC family to a cultivar (Fig 5B).

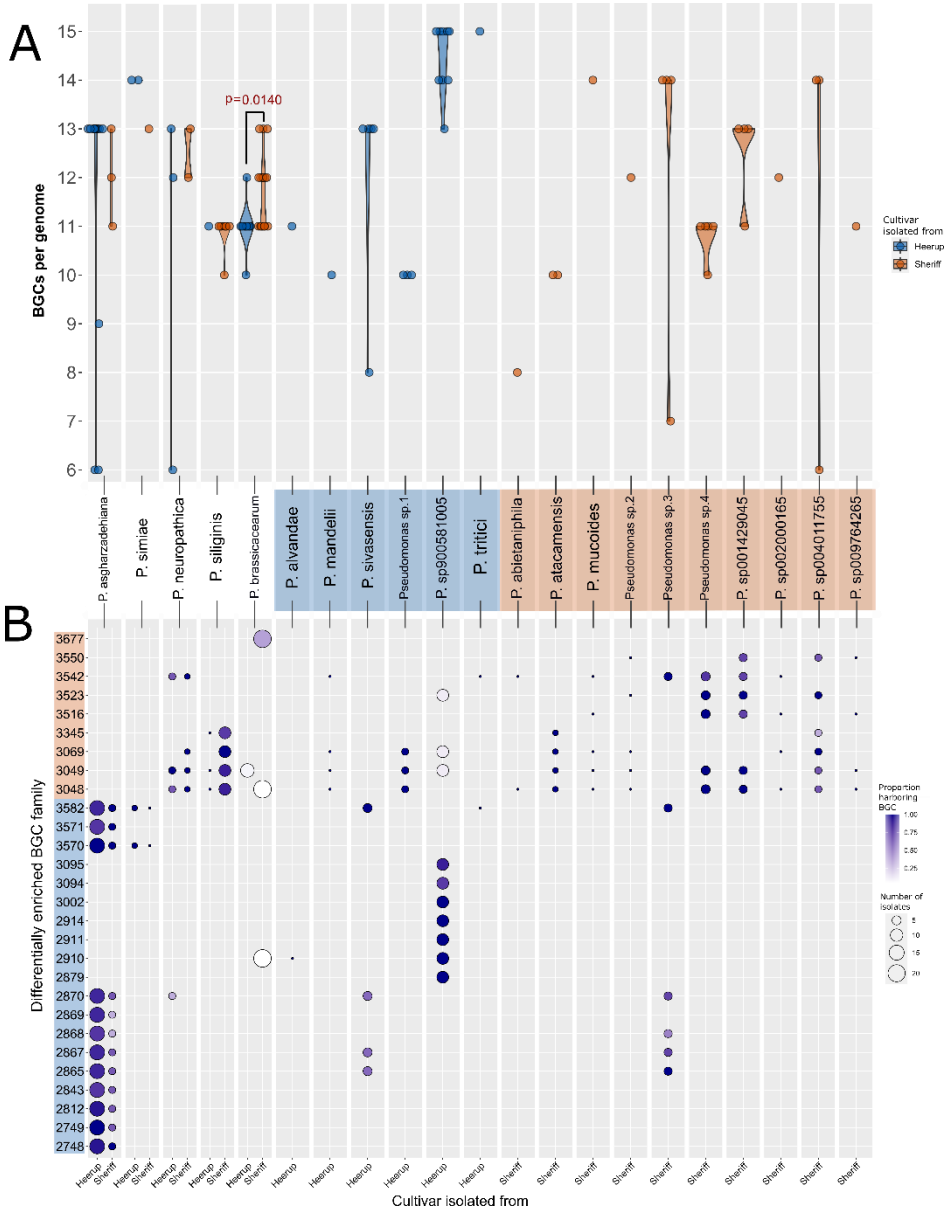

451

452 **Figure 5. Distribution of BGCs in the species found in the *Pseudomonas* strain library. X-axis**
453 **highlight box represents if the species is found only in Heerup (blue) or Sheriff (orange).** A)
454 Number of BGCs per genome. True data points are overlaid the violin plot as filled circles. Significant
455 differences in average BGCs per genome of a species between cultivars was calculated using the
456 two-sided Wilcoxon Rank Sum test for the species *P. brassicacearum*, *P. siliginis*, and *P.*
457 *asgharzadehiana,* and only $p < 0.05$ are displayed. B) Proportion of isolates of each species harboring
458 the BGC family that is differentially enriched between Heerup and Sheriff. The Y-axis highlight box
459 represents if the BGC family is enriched in Heerup (blue) or Sheriff (orange).

460

461 ### 5) Root scanning correlates Sheriff *Pseudomonas* community to thinner root diameter

462 Culture-dependent and culture-independent 16S rRNA gene sequencing indicated that the Sheriff
463 cultivar harbors a more diverse *Pseudomonas* population. To test the hypothesis that a more diverse
464 *Pseudomonas* community would correlate with a thinner root diameter, we scanned the roots of
465 four-week old Heerup and Sheriff plants and measured the root diameter of the system. The ANOVA
466 model showed significant interaction between cultivar and percentage of root system in each root
467 class (p = 3.81e-5). Sheriff had a higher percentage of thinner roots between 0.2-0.3 mm, while
468 Heerup had a higher percentage of thicker roots above 0.5 mm (two-sided Student T test, $p < 0.05$)
469 (Figure 6). This contributed to the thinner average root diameter of Sheriff (0.35 ± 0.03 mm)
470 compared to Heerup (0.40 ± 0.03 mm) (two-sided Student T test, p = 0.0026).

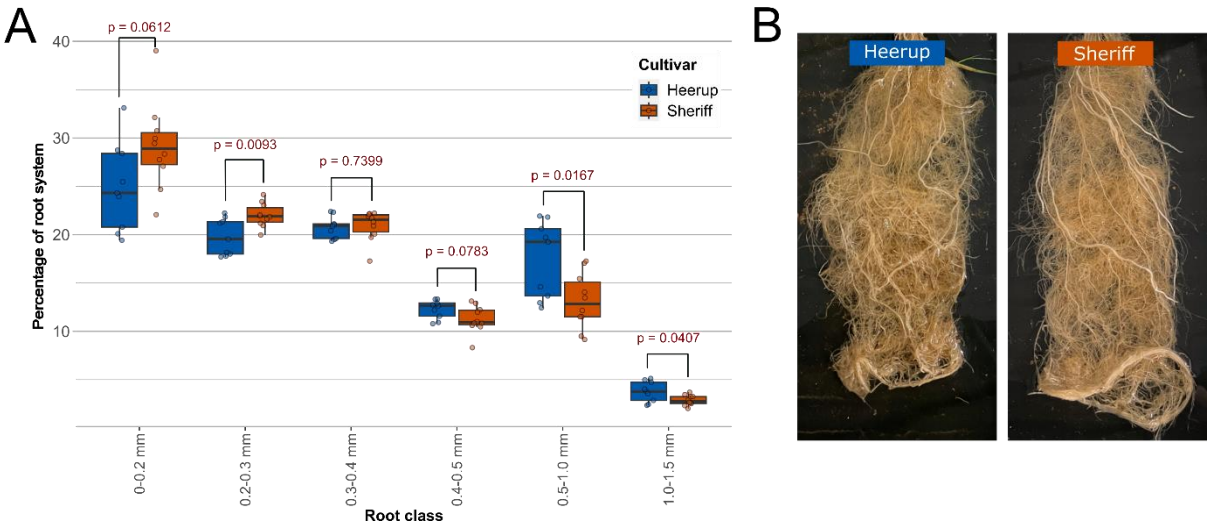

471

472 **Figure 6. Root scanning was performed on four-week old plants to measure root morphology**
473 **parameters.** A) Root system composition of Heerup and Sheriff divided into six root diameter
474 ranges. The box plots display the median, the two hinges (25th and 75th percentile), and the upper
475 and lower whiskers (extending to the largest and smallest values no further than 1.5 times the
476 interquartile range). True data points are overlaid the boxplot as filled circles. P values derived from
477 the two-sided Student T test are shown. B) Representative images of washed Heerup and Sheriff
478 root systems after four weeks of growth.

479

480 ## Discussion

481 Our study provides an in-depth insight into the microdiversity of *Pseudomonas* communities in two
482 commercially available cultivars of winter wheat with contrasting susceptibility to the fungal
483 pathogen *F. culmorum* under field conditions. With 373 isolates and 112 genomes, this is to our
484 knowledge the largest study to characterize *Pseudomonas* microdiversity and critically the first to do
485 so in wheat, a major global supplier of calories (Erenstein et al., 2022). In field-grown wheat
486 rhizospheres, *Pseudomonas* are present in low abundances (Mauchline et al., 2015; Simonin et al.,
487 2020), but successfully shape the assembly of the rhizosphere microbiome (Garrido-Sanz et al.,
488 2023; Getzke et al., 2023) and antagonize pathogens (Hong et al., 2023; Lv et al., 2023). As indicated
489 by the results of our work, microdiversity of *Pseudomonas* taxonomy in plant-associated
490 microbiomes can be extensive, with 22 species and 48 strains found from 373 isolates and 70 ASVS
491 revealed in long-read 16S rRNA amplicon sequencing. Previous work in cocoyam classified 134
492 *Pseudomonas* isolates into seven phylogenetic subgroups (Oni et al., 2019), and in potato, seven

phylogenetic subgroups were represented across 69 isolates (Pacheco-Moreno et al., 2021). Interestingly, the low-abundance ASVs were different from the low-abundance isolates, indicating unique biases in both culturing and sequencing. Thus, we suggest that both approaches are needed to capture the full picture of *Pseudomonas* microdiversity in the rhizoplane.

As the *Pseudomonas* genus can be influenced by wheat cultivar (Mauchline et al., 2015; Zheng et al., 2023), and it is known that plant genotype can dictate microbiome assembly (Spor et al., 2020; Zheng et al., 2023), we made a general hypothesis that *Pseudomonas* taxonomic and functional microdiversity is cultivar-dependent. Specifically, we hypothesized that this would result in the resistant cultivar, Sheriff, having increased diversity compared to the susceptible Heerup cultivar, since increasing intraspecies diversity is beneficial for plant health (Hu et al., 2016; Jousset et al., 2011; Li et al., 2023). In the present work, both culture-based and sequencing approaches indicated that species within the *Pseudomonas* genus can be enriched in one or the other wheat cultivars. For example, the species *P. asgharzadehiana* was five times more abundant in the Heerup cultivar, ten of the 19 identifed species were cultured only from Sheriff cultivar, and eight ASVS were enriched in Sheriff amplicons. It is not the first time that it has been reported that plants can differentiate between phylogenetically similar bacteria (Thoms et al., 2023; Zhang & Kong, 2022). Culturable and *in silico* community analysis established that the Sheriff cultivar harbors a more taxonomically diverse and unique *Pseudomonas* community, in support of our hypothesis. While not fully explored in this work, it may not be coincidental that the resistant cultivar Sheriff harbors two times the number of unique *Pseudomonas* strains compared to its susceptible relative. Further microbiome analyses on susceptible versus resistant wheat cultivars against additional pathogens would support the beneficial effect of taxonomic microdiversity on plant health.

We also sought to demonstrate that functional microdiversity within the *Pseudomonas* genus can be cultivar-specific. Many microbial functionalities can be subject to microdiversity (Larkin & Martiny, 2017), and functional microdiversity is not rare within genera (Scales et al., 2023; Ustick et al., 2023). In this experiment, there were several instances of genomic loci enriched in one cultivar or the other, but many of the functions gained or lost remain unclear due to extensive dark matter in microbial genomes (Gavriilidou et al., 2022). The distribution of BGC families also revealed potential cultivar-specific functions within the pseudomonads. BGC families are one way to group architecturally similar BGCs that can be linked to a natural product chemotype (Navarro-Muñoz et al., 2020), and thus, may be used as a proxy for different potential functions. Upon further analysis, this result stemmed from the allocation of specific pseudomonads to Heerup or Sheriff cultivar. For example, the enrichment of the BGC FAM_3049 in Sheriff is reflected by the increased presence of several species carrying this BGC in Sheriff, while the enrichment of BGC FAM_2749 in Heerup is driven by the higher abundance of *P. asgharzadehiana* in Heerup. In one case, it stemmed from cultivar-dependent interspecies microdiversity. The species *P. brassicacearum* carried BGC FAM_3677 only when it was isolated from the Sheriff cultivar. Interestingly, *P. brassicacearum* was the only species where average number of BGC per genome was affected by cultivar, with Sheriff P. *brassicacearum* strains harboring more BGCs per genome in comparison to their Heerup counterparts. Further genome sequencing of Heerup and Sheriff rhizosphere pseudomonads would confirm this interesting trend. It is also still up for debate how and why pseudomonads carrying these BGC families are found on their respective cultivar, especially since most of the BGCs in the strain library are unclassified beyond their product class. Further work in this area could resolve how

536 crops recruit bacteria producing certain metabolites to their microbiome, a mechanism previously
537 suggested but poorly understood (Liu et al., 2021; Feng et al., 2023; K. Yang et al., 2023).

538 Interestingly, the less taxonomically diverse Heerup pseudomonads demonstrated increased
539 biosynthetic functional diversity, boasting 19 enriched BGC families of 11 different product types
540 while Sheriff only had nine families of five product types. Our results suggest that the preferential
541 colonization of the highly biosynthetic species *P. asgharzadehiana* on Heerup underpins this result.
542 This goes against the preconceived notion that increased taxonomic microdiversity results in
543 increased functional microdiversity. This may be a conserved characteristic; in soil, bacterial
544 taxonomic and functional diversity are negatively correlated (C. Wang et al., 2023).

545 Hence, our data demonstrate the ability of the wheat cultivar to influence *Pseudomonas* taxonomic
546 and functional microdiversity. Our collection of cultivar-specific isolates and the functional potential
547 within their genomes can act as a tool to further dissect high-resolution plant-microbe interactions,
548 as 16S rRNA gene sequences alone are not enough to reveal intragenus microdiversity (Jaspers &
549 Overmann, 2004; Kiepas et al., 2023; Stevens et al., 2023; Chiniquy et al., 2021; Ordon et al., 2024).
550 Exploration of these cultivar-dependent genomic loci may reveal insights regarding the specificity of
551 plant-microbe interactions at the species level. Ultimately, unraveling this interaction can allow for
552 designer crops that harbor microbial metabolites which can be used for increased resilience in the
553 face of challenging growing conditions. Cultivar-dependent microdiversity resulted in the resistant
554 cultivar, Sheriff, being more diverse than the susceptible Heerup cultivar in *Pseudomonas* taxonomy
555 but not function. We suggest that microdiversity should be explored as a potential metric for the
556 health and productivity of plant microbiomes, but the relationship between taxonomy and function
557 remains a confounding factor on the mechanism underpinning taxonomic diversity and pathogen
558 suppression.

559 We also hypothesized that the more taxonomically diverse cultivar of wheat would have a thinner
560 average root diameter, and in support of this hypothesis, we saw that the more diverse Sheriff
561 cultivar had a thinner average root diameter and a higher proprotion of thinner roots compared to
562 Heerup. This contributes to the growing body of literature that for both woody and herbaceous
563 plant species, thinner roots, or a root system dominated by fine roots, promote a more diverse
564 bacterial community (Fleishman et al., 2023; Luo et al., 2021; Pervaiz et al., 2020; Saleem et al.,
565 2018; Zai et al., 2021). Nevertheless, it is not possible at this time to attribute the differences in
566 *Pseudomonas* communities to the root morphology of the cultivars, since the cultivars are
567 genetically distinct. Other factors including root exudation and plant genes are certainly at play
568 (Sasse et al., 2018; Y. Song et al., 2021). Still, root diameter and root morphology as a whole might
569 play a previously unexplored role in microbial community composition, as we have suggested
570 previously (Herms et al., 2022), and deserve further evaluation.

571 Our last hypothesis predicted that the cultivar resistant to *F. culmorum* infection in the field, Sheriff,
572 would harbor enriched antifungal activity, genes linked to antifungal activity, and BGCs for antifungal
573 secondary metabolites within its *Pseudomonas* community. *Pseudomonas* communities are often
574 implicated in disease suppression, even when grouped together at the genus level (Hong et al., 2023;
575 Lv et al., 2023; Qiu et al., 2022). To test this, we screened the strain library for antifungal activity and
576 the genomes for antifungal genes and BGCs. We found more *in vitro* antifungal activity in the Sheriff
577 isolates. Isolates that were positive for fungal inhibition also mapped to ASVs that were enriched in
578 the Sheriff microbiome during amplicon sequencing. A chitinase from the family GH19 was also

enriched in Sheriff isolates. The GH19 family, originating from plants but also found in some bacteria including *Pseudomonas* (Ren et al., 2022), are notable for their prolific antifungal activity (Watanabe et al., 1999). We also found a predicted *P. fluorescens*-type pyoverdine BGC that was enriched in Sheriff pseudomonads. Pyoverdines are beneficial in enabling pseudomonads to prevent the growth of fungal pathogens via competition for iron (Dutta et al., 2020; S. Gu et al., 2020). The BGC for another antagonistic metabolite, 2,4-DAPG, was found equally distributed between the two cultivars; however, antifungal activity of 2,4-DAPG against *Fusarium* is not equal amongst all producing *Pseudomonas* strains (Sharifi-Tehrani et al., 1998). Neither of the two CLPs found in the strain library, viscosin and lokisin, were enriched in either Heerup or Sheriff cultivar. Viscosin is the most common CLP in *Pseudomonas* (Cesa-Luna et al., 2023) and is known for its surfactant rather than antifungal activity (Geudens & Martins, 2018). On the other hand, lokisin has antifungal activity (Y. Gu et al., 2020) yet is also a CLP commonly associated to Danish soil pseudomonads (Nielsen et al., 2002). Additional BGCs found equally between both cultivars include tabtoxin, the precursor for the antibiotic tabtoxinine β-lactam (Kinscherf & Willis, 2005) and 3-thialglutatmate, which may interact with plant glutamate signaling (Ting et al., 2019). Taken together, we found an enrichment of antifungal strains in the Sheriff cultivar co-occurring with an enrichment of the GH19 chitinase and a pyoverdine BGC, while other potentially antifungal BGCs were equally distributed across cultivars. Thus, one potential mechanism for microbiome-mediated *Fusarium* resistance of the Sheriff cultivar could be chitinase activity and/or pyoverdine production. Further studies with knockouts in chitinase and pyoverdine production would reveal their true effect on *F. culmorum* growth in this wheat cultivar.

Conclusion

The rhizosphere microbiome is a key determinant of plant health, and ongoing research aims to unravel the mechanisms by which crops recruit beneficial microbes to their roots. In the current work, we demonstrated cultivar-dependent *Pseudomonas* taxonomic and functional microdiversity, revealing the importance of fine-scale microbial sampling in order to understand differences in the microbiomes of closely related plants. Through a sampling campaign of over 300 *Pseudomonas* isolates, we uncovered a number of species and strains that preferentially colonize one wheat cultivar over the other. By sequencing 112 genomes of the strain collection, we saw that antifungal activity and antifungal genes were enriched in *Pseudomonas* isolated from the *Fusarium* resistant cultivar, while highly biosynthetic pseudomonads were harbored by the other cultivar. We demonstrate that the status quo of grouping together highly diverse genera, such as *Pseudomonas*, in sampling approaches overlooks crucial differences in microbial functional activity. Failing to consider the importance of microdiversity in shaping the composition and function of the rhizosphere microbiome conceals the true potential of root-associated microbial communities and should be a focus area in future plant holobiont research.

Conflict of Interests

The authors report no conflicts of interest.

Acknowledgements

Thanks to Dorette Müller-Stöver and Marie Louise Bornø, University of Copenhagen, for supplying experimental soils and measurements of soil chemical characteristics. The *Fusarium culmorum* strain was kindly provided by Birgit Jensen, University of Copenhagen. Thanks to our group members Kitzia Yashvelt Molina Zamudio and Dorthe Thybo Ganzhorn for their support with the sampling. This study was funded by the Novo Nordisk Foundation (Grant number: NNF19SA0059360).

References

Alsohim, A. S., Taylor, T. B., Barrett, G. A., Gallie, J., Zhang, X. X., Altamirano-Junqueira, A. E., Johnson, L. J., Rainey, P. B., & Jackson, R. W. (2014). The biosurfactant viscosin produced by Pseudomonas fluorescensSBW25 aids spreading motility and plant growth promotion. *Environmental Microbiology*, *16*(7), 2267–2281. https://doi.org/10.1111/1462-2920.12469

Altschul, S. F., Madden, T. L., Schäffer, A. A., Zhang, J., Zhang, Z., Miller, W., & Lipman, D. J. (1997). Gapped BLAST and PSI-BLAST: A new generation of protein database search programs. *Nucleic Acids Research*, *25*(17), 3389–3402. https://doi.org/10.1093/nar/25.17.3389

Bai, B., Liu, W., Qiu, X., Zhang, J., Zhang, J., & Bai, Y. (2022). The root microbiome: Community assembly and its contributions to plant fitness. *Journal of Integrative Plant Biology*, *64*(2), 230–243. https://doi.org/10.1111/jipb.13226

Benjamini, Y., & Hochberg, Y. (1995). Controlling the False Discovery Rate: A Practical and Powerful Approach to Multiple Testing. *Journal of the Royal Statistical Society: Series B (Methodological)*, *57*(1), 289–300. https://doi.org/10.1111/j.2517-6161.1995.tb02031.x

Berg, G., Köberl, M., Rybakova, D., Müller, H., Grosch, R., & Smalla, K. (2017). Plant microbial diversity is suggested as the key to future biocontrol and health trends. *FEMS Microbiology Ecology*, *93*(5), 1–9. https://doi.org/10.1093/femsec/fix050

Bodour, A. A., & Miller-Maier, R. M. (1998). Application of a modified drop-collapse technique for surfactant quantitation and screening of biosurfactant-producing microorganisms. *Journal of Microbiological Methods*, *32*(3), 273–280. https://doi.org/10.1016/S0167-7012(98)00031-1

Capella-Gutiérrez, S., Silla-Martínez, J. M., & Gabaldón, T. (2009). trimAl: A tool for automated alignment trimming in large-scale phylogenetic analyses. *Bioinformatics*, *25*(15), 1972–1973. https://doi.org/10.1093/bioinformatics/btp348

Caporaso, J. G., Kuczynski, J., Stombaugh, J., Bittinger, K., Bushman, F. D., Costello, E. K., Fierer, N., Peña, A. G., Goodrich, J. K., Gordon, J. I., Huttley, G. A., Kelley, S. T., Knights, D., Koenig, J. E., Ley, R. E., Lozupone, C. A., McDonald, D., Muegge, B. D., Pirrung, M., … Knight, R. (2010). QIIME allows analysis of high-throughput community sequencing data. *Nature Methods*, *7*(5), Article 5. https://doi.org/10.1038/nmeth.f.303

Castresana, J. (2000). Selection of Conserved Blocks from Multiple Alignments for Their Use in Phylogenetic Analysis. *Molecular Biology and Evolution*, *17*(4), 540–552. https://doi.org/10.1093/oxfordjournals.molbev.a026334

Cesa-Luna, C., Geudens, N., Girard, L., De Roo, V., Maklad, H. R., Martins, J. C., Höfte, M., & De Mot, R. (2023). Charting the Lipopeptidome of Nonpathogenic Pseudomonas. *mSystems*, *0*(0), e00988-22. https://doi.org/10.1128/msystems.00988-22

Chao, A. (1984). Nonparametric Estimation of the Number of Classes in a Population. *Scandinavian Journal of Statistics*, *11*(4), 265–270.

Chaumeil, P.-A., Mussig, A. J., Hugenholtz, P., & Parks, D. H. (2020). GTDB-Tk: A toolkit to classify genomes with the Genome Taxonomy Database. *Bioinformatics*, *36*(6), 1925–1927. https://doi.org/10.1093/bioinformatics/btz848

Chiniquy, D., Barnes, E. M., Zhou, J., Hartman, K., Li, X., Sheflin, A., Pella, A., Marsh, E., Prenni, J., Deutschbauer, A. M., Schachtman, D. P., & Tringe, S. G. (2021). Microbial Community Field Surveys Reveal Abundant Pseudomonas Population in Sorghum Rhizosphere Composed of Many Closely Related Phylotypes. *Frontiers in Microbiology*, *12*. https://doi.org/10.3389/fmicb.2021.598180

Clarke, K. R. (1993). Non-parametric multivariate analyses of changes in community structure. *Australian Journal of Ecology*, *18*(1), 117–143. https://doi.org/10.1111/j.1442-9993.1993.tb00438.x

De Coster, W., D'Hert, S., Schultz, D. T., Cruts, M., & Van Broeckhoven, C. (2018). NanoPack: Visualizing and processing long-read sequencing data. *Bioinformatics*, *34*(15), 2666–2669. https://doi.org/10.1093/bioinformatics/bty149

Dubey, M., Hadadi, N., Pelet, S., Carraro, N., Johnson, D. R., & van der Meer, J. R. (2021). Environmental connectivity controls diversity in soil microbial communities. *Communications Biology*, *4*(1), Article 1. https://doi.org/10.1038/s42003-021-02023-2

Durán, D., Bernal, P., Vazquez-Arias, D., Blanco-Romero, E., Garrido-Sanz, D., Redondo-Nieto, M., Rivilla, R., & Martín, M. (2021). Pseudomonas fluorescens F113 type VI secretion systems mediate bacterial killing and adaption to the rhizosphere microbiome. *Scientific Reports*, *11*(1), Article 1. https://doi.org/10.1038/s41598-021-85218-1

Dutta, S., Yu, S.-M., & Lee, Y. H. (2020). Assessment of the Contribution of Antagonistic Secondary Metabolites to the Antifungal and Biocontrol Activities of Pseudomonas fluorescens NBC275. *The Plant Pathology Journal*, *36*(5), 491–496. https://doi.org/10.5423/PPJ.FT.08.2020.0149

Edgar, R. C. (2004). MUSCLE: Multiple sequence alignment with high accuracy and high throughput. *Nucleic Acids Research*, *32*(5), 1792–1797. https://doi.org/10.1093/nar/gkh340

Edgar, R. C. (2010). Search and clustering orders of magnitude faster than BLAST. *Bioinformatics*, *26*(19), 2460–2461. https://doi.org/10.1093/bioinformatics/btq461

Edgar, R. C. (2016). *UNOISE2: Improved error-correction for Illumina 16S and ITS amplicon sequencing* (p. 081257). bioRxiv. https://doi.org/10.1101/081257

Edgar, R. C. (2018). Updating the 97% identity threshold for 16S ribosomal RNA OTUs. *Bioinformatics*, *34*(14), 2371–2375. https://doi.org/10.1093/bioinformatics/bty113

Eren, A. M., Kiefl, E., Shaiber, A., Veseli, I., Miller, S. E., Schechter, M. S., Fink, I., Pan, J. N., Yousef, M., Fogarty, E. C., Trigodet, F., Watson, A. R., Esen, Ö. C., Moore, R. M., Clayssen, Q., Lee, M. D., Kivenson, V., Graham, E. D., Merrill, B. D., … Willis, A. D. (2021). Community-led, integrated, reproducible multi-omics with anvi'o. *Nature Microbiology*, *6*(1), Article 1. https://doi.org/10.1038/s41564-020-00834-3

Erenstein, O., Jaleta, M., Mottaleb, K. A., Sonder, K., Donovan, J., & Braun, H.-J. (2022). Global Trends in Wheat Production, Consumption and Trade. In M. P. Reynolds & H.-J. Braun (Eds.), *Wheat Improvement: Food Security in a Changing Climate* (pp. 47–66). Springer International Publishing. https://doi.org/10.1007/978-3-030-90673-3_4

Feng, H., Fu, R., Luo, J., Hou, X., Gao, K., Su, L., Xu, Y., Miao, Y., Liu, Y., Xu, Z., Zhang, N., Shen, Q., Xun, W., & Zhang, R. (2023). Listening to plant's Esperanto via root exudates: Reprogramming the functional expression of plant growth-promoting rhizobacteria. *New Phytologist*, *239*(6), 2307–2319. https://doi.org/10.1111/nph.19086

Fleishman, S. M., Centinari, M., Bell, T. H., & Eissenstat, D. M. (2023). Assessing microbial communities across the fine root landscape. *Journal of Experimental Botany*, erad019. https://doi.org/10.1093/jxb/erad019

Garrido-Sanz, D., Čaušević, S., Vacheron, J., Heiman, C. M., Sentchilo, V., van der Meer, J. R., & Keel, C. (2023). Changes in structure and assembly of a species-rich soil natural community with contrasting nutrient availability upon establishment of a plant-beneficial Pseudomonas in

the wheat rhizosphere. *Microbiome*, *11*(1), 214. https://doi.org/10.1186/s40168-023-01660-5

Gavriilidou, A., Kautsar, S. A., Zaburannyi, N., Krug, D., Müller, R., Medema, M. H., & Ziemert, N. (2022). Compendium of specialized metabolite biosynthetic diversity encoded in bacterial genomes. *Nature Microbiology*, *7*(5), Article 5. https://doi.org/10.1038/s41564-022-01110-2

Getzke, F., Hassani, M. A., Crüsemann, M., Malisic, M., Zhang, P., Ishigaki, Y., Böhringer, N., Jiménez Fernández, A., Wang, L., Ordon, J., Ma, K.-W., Thiergart, T., Harbort, C. J., Wesseler, H., Miyauchi, S., Garrido-Oter, R., Shirasu, K., Schäberle, T. F., Hacquard, S., & Schulze-Lefert, P. (2023). Cofunctioning of bacterial exometabolites drives root microbiota establishment. *Proceedings of the National Academy of Sciences*, *120*(15), e2221508120. https://doi.org/10.1073/pnas.2221508120

Geudens, N., & Martins, J. C. (2018). Cyclic lipodepsipeptides from Pseudomonas spp. - Biological Swiss-Army knives. *Frontiers in Microbiology*, *9*(AUG), 1–18. https://doi.org/10.3389/fmicb.2018.01867

Girard, L., Lood, C., Höfte, M., Vandamme, P., Rokni-Zadeh, H., van Noort, V., Lavigne, R., & De Mot, R. (2021). The Ever-Expanding Pseudomonas Genus: Description of 43 New Species and Partition of the Pseudomonas putida Group. *Microorganisms*, *9*(8), Article 8. https://doi.org/10.3390/microorganisms9081766

Gross, H., & Loper, J. E. (2009). Genomics of secondary metabolite production by Pseudomonas spp. *Natural Product Reports*, *26*(11), 1408–1446. https://doi.org/10.1039/b817075b

Gu, S., Wei, Z., Shao, Z., Friman, V.-P., Cao, K., Yang, T., Kramer, J., Wang, X., Li, M., Mei, X., Xu, Y., Shen, Q., Kümmerli, R., & Jousset, A. (2020). Competition for iron drives phytopathogen control by natural rhizosphere microbiomes. *Nature Microbiology*, *5*(8), Article 8. https://doi.org/10.1038/s41564-020-0719-8

Gu, Y., Ma, Y.-N., Wang, J., Xia, Z., & Wei, H.-L. (2020). Genomic insights into a plant growth-promoting Pseudomonas koreensis strain with cyclic lipopeptide-mediated antifungal activity. *MicrobiologyOpen*, *9*(9), e1092. https://doi.org/10.1002/mbo3.1092

Hennessy, R. C., Dichmann, S. I., Martens, H. J., Zervas, A., & Stougaard, P. (2020). Serratia inhibens sp. Nov., a new antifungal species isolated from potato (Solanum tuberosum). *International Journal of Systematic and Evolutionary Microbiology*, *70*(7), 4204–4211. https://doi.org/10.1099/ijsem.0.004270

Herms, C. H., Hennessy, R. C., Bak, F., Dresbøll, D. B., & Nicolaisen, M. H. (2022). Back to our roots: Exploring the role of root morphology as a mediator of beneficial plant–microbe interactions. *Environmental Microbiology*, *00*. https://doi.org/10.1111/1462-2920.15926

Hong, S., Yuan, X., Yang, J., Yang, Y., Jv, H., Li, R., Jia, Z., & Ruan, Y. (2023). Selection of rhizosphere communities of diverse rotation crops reveals unique core microbiome associated with reduced banana Fusarium wilt disease. *New Phytologist*, *238*(5), 2194–2209. https://doi.org/10.1111/nph.18816

Hu, J., Wei, Z., Friman, V. P., Gu, S. H., Wang, X. F., Eisenhauer, N., Yang, T. J., Ma, J., Shen, Q. R., Xu, Y. C., & Jousset, A. (2016). Probiotic diversity enhances rhizosphere microbiome function and plant disease suppression. *mBio*, *7*(6), 1–8. https://doi.org/10.1128/mBio.01790-16

Huang, Y., Sheth, R. U., Zhao, S., Cohen, L. A., Dabaghi, K., Moody, T., Sun, Y., Ricaurte, D., Richardson, M., Velez-Cortes, F., Blazejewski, T., Kaufman, A., Ronda, C., & Wang, H. H. (2023). High-throughput microbial culturomics using automation and machine learning. *Nature Biotechnology*, 1–10. https://doi.org/10.1038/s41587-023-01674-2

Ilmi, M., Putri, L. K., Muhamad, A. A. K., Cholishoh, A., & Ardiansyah, S. A. (2019). Use of Mung Bean Sprout (Tauge) as Alternative Fungal Growth Medium. *Journal of Physics: Conference Series*, *1241*(1), 012015. https://doi.org/10.1088/1742-6596/1241/1/012015

Jaspers, E., & Overmann, J. (2004). Ecological Significance of Microdiversity: Identical 16S rRNA Gene Sequences Can Be Found in Bacteria with Highly Divergent Genomes and Ecophysiologies. *Applied and Environmental Microbiology*, *70*(8), 4831–4839. https://doi.org/10.1128/AEM.70.8.4831-4839.2004

Jørgensen, L. N., Heick, T. M., Abuley, I. K., Kudsk, P., & Hansen Kemezys, A. (2023). *Applied Crop Protection 2022* (Research Dissemination 216). Aarhus University.

Jørgensen, L. N., Heick, T. M., Abuley, I. K., Mathiassen, S., Jensen, P. K., Kristjansen, H. S., & Hartvig, P. (2020). *Applied Crop Protection 2019* (Research Dissemination 167). Aarhus University.

Jousset, A., Schulz, W., Scheu, S., & Eisenhauer, N. (2011). Intraspecific genotypic richness and relatedness predict the invasibility of microbial communities. *The ISME Journal*, *5*(7), 1108–1114. https://doi.org/10.1038/ismej.2011.9

Kiepas, A. B., Hoskisson, P. A., & Pritchard, L. (2023). *16S rRNA phylogeny and clustering is not a reliable proxy for genome-based taxonomy in Streptomyces* (p. 2023.08.15.553377). bioRxiv. https://doi.org/10.1101/2023.08.15.553377

King, W. L., Yates, C. F., Cao, L., O'Rourke-Ibach, S., Fleishman, S. M., Richards, S. C., Centinari, M., Hafner, B. D., Goebel, M., Bauerle, T., Kim, Y.-M., Nicora, C. D., Anderton, C. R., Eissenstat, D. M., & Bell, T. H. (2023). Functionally discrete fine roots differ in microbial assembly, microbial functional potential, and produced metabolites. *Plant, Cell & Environment*, *46*(12), 3919–3932. https://doi.org/10.1111/pce.14705

Kinscherf, T. G., & Willis, D. K. (2005). The Biosynthetic Gene Cluster for the β-Lactam Antibiotic Tabtoxin in Pseudomonas syringae. *The Journal of Antibiotics*, *58*(12), 817–821. https://doi.org/10.1038/ja.2005.109

Kolmogorov, M., Yuan, J., Lin, Y., & Pevzner, P. A. (2019). Assembly of long, error-prone reads using repeat graphs. *Nature Biotechnology*, *37*(5), Article 5. https://doi.org/10.1038/s41587-019-0072-8

Larkin, A. A., & Martiny, A. C. (2017). Microdiversity shapes the traits, niche space, and biogeography of microbial taxa. *Environmental Microbiology Reports*, *9*(2), 55–70. https://doi.org/10.1111/1758-2229.12523

Li, J., Yang, C., Jousset, A., Yang, K., Wang, X., Xu, Z., Yang, T., Mei, X., Zhong, Z., Xu, Y., Shen, Q., Friman, V.-P., & Wei, Z. (2023). Engineering multifunctional rhizosphere probiotics using consortia of Bacillus amyloliquefaciens transposon insertion mutants. *eLife*, *12*, e90726. https://doi.org/10.7554/eLife.90726

Lin, Y., Yuan, J., Kolmogorov, M., Shen, M. W., Chaisson, M., & Pevzner, P. A. (2016). Assembly of long error-prone reads using de Bruijn graphs. *Proceedings of the National Academy of Sciences*, *113*(52), E8396–E8405. https://doi.org/10.1073/pnas.1604560113

Liu, H., Li, J., Carvalhais, L. C., Percy, C. D., Prakash Verma, J., Schenk, P. M., & Singh, B. K. (2021). Evidence for the plant recruitment of beneficial microbes to suppress soil-borne pathogens. *New Phytologist*, *229*(5), 2873–2885. https://doi.org/10.1111/nph.17057

Loper, J. E., Hassan, K. A., Mavrodi, D. V., Davis, E. W., Lim, C. K., Shaffer, B. T., Elbourne, L. D. H., Stockwell, V. O., Hartney, S. L., Breakwell, K., Henkels, M. D., Tetu, S. G., Rangel, L. I., Kidarsa, T. A., Wilson, N. L., van de Mortel, J. E., Song, C., Blumhagen, R., Radune, D., … Paulsen, I. T. (2012). Comparative genomics of plant-associated pseudomonas spp.: Insights into diversity and inheritance of traits involved in multitrophic interactions. *PLoS Genetics*, *8*(7). https://doi.org/10.1371/journal.pgen.1002784

Lopes, L. D., Davis, E. W., Pereira e Silva, M. de C., Weisberg, A. J., Bresciani, L., Chang, J. H., Loper, J. E., & Andreote, F. D. (2018). Tropical soils are a reservoir for fluorescent Pseudomonas spp. Biodiversity. *Environmental Microbiology*, *20*(1), 62–74. https://doi.org/10.1111/1462-2920.13957

Luo, W., Zai, X., Sun, J., Li, D., Li, Y., Li, G., Wei, G., & Chen, W. (2021). Coupling Root Diameter With Rooting Depth to Reveal the Heterogeneous Assembly of Root-Associated Bacterial Communities in Soybean. *Frontiers in Microbiology*, *12*(December). https://doi.org/10.3389/fmicb.2021.783563

Lv, N., Tao, C., Ou, Y., Wang, J., Deng, X., Liu, H., Shen, Z., Li, R., & Shen, Q. (2023). Root-Associated Antagonistic Pseudomonas spp. Contribute to Soil Suppressiveness against Banana Fusarium Wilt Disease of Banana. *Microbiology Spectrum*, *0*(0), e03525-22. https://doi.org/10.1128/spectrum.03525-22

Mauchline, T. H., Chedom-Fotso, D., Chandra, G., Samuels, T., Greenaway, N., Backhaus, A., Mcmillan, V., Canning, G., Powers, S. J., Hammond-Kosack, K. E., Hirsch, P. R., Clark, I. M., Mehrabi, Z., Roworth, J., Burnell, J., & Malone, J. G. (2015). An analysis of Pseudomonas genomic diversity in take-all infected wheat fields reveals the lasting impact of wheat cultivars on the soil microbiota. *Environmental Microbiology*, *17*(11), 4764–4778. https://doi.org/10.1111/1462-2920.13038

Mauchline, T. H., & Malone, J. G. (2017). Life in earth – the root microbiome to the rescue? *Current Opinion in Microbiology*, *37*, 23–28. https://doi.org/10.1016/j.mib.2017.03.005

Medema, M. H., Blin, K., Cimermancic, P., de Jager, V., Zakrzewski, P., Fischbach, M. A., Weber, T., Takano, E., & Breitling, R. (2011). antiSMASH: Rapid identification, annotation and analysis of secondary metabolite biosynthesis gene clusters in bacterial and fungal genome sequences. *Nucleic Acids Research*, *39*(suppl_2), W339–W346. https://doi.org/10.1093/nar/gkr466

Mesny, F., Hacquard, S., & Thomma, B. P. (2023). Co-evolution within the plant holobiont drives host performance. *EMBO Reports*, *24*(9), e57455. https://doi.org/10.15252/embr.202357455

Minh, B. Q., Schmidt, H. A., Chernomor, O., Schrempf, D., Woodhams, M. D., von Haeseler, A., & Lanfear, R. (2020). IQ-TREE 2: New Models and Efficient Methods for Phylogenetic Inference in the Genomic Era. *Molecular Biology and Evolution*, *37*(5), 1530–1534. https://doi.org/10.1093/molbev/msaa015

Moore, L. R., Rocap, G., & Chisholm, S. W. (1998). Physiology and molecular phylogeny of coexisting Prochlorococcus ecotypes. *Nature*, *393*(6684), Article 6684. https://doi.org/10.1038/30965

Navarro-Muñoz, J. C., Selem-Mojica, N., Mullowney, M. W., Kautsar, S. A., Tryon, J. H., Parkinson, E. I., De Los Santos, E. L. C., Yeong, M., Cruz-Morales, P., Abubucker, S., Roeters, A., Lokhorst, W., Fernandez-Guerra, A., Cappelini, L. T. D., Goering, A. W., Thomson, R. J., Metcalf, W. W., Kelleher, N. L., Barona-Gomez, F., & Medema, M. H. (2020). A computational framework to explore large-scale biosynthetic diversity. *Nature Chemical Biology*, *16*(1), Article 1. https://doi.org/10.1038/s41589-019-0400-9

Nielsen, T. H., Sørensen, D., Tobiasen, C., Andersen, J. B., Christophersen, C., Givskov, M., & Sørensen, J. (2002). Antibiotic and Biosurfactant Properties of Cyclic Lipopeptides Produced by Fluorescent Pseudomonas spp. From the Sugar Beet Rhizosphere. *Applied and Environmental Microbiology*, *68*(7), 3416–3423. https://doi.org/10.1128/AEM.68.7.3416-3423.2002

Oksanen, J., Simpson, G. L., Blanchet, F. G., Kindt, R., Legendre, P., Minchin, P. R., O'Hara, R. B., Solymos, P., Stevens, M. H. H., Szoecs, E., Wagner, H., Barbour, M., Bedward, M., Bolker, B., Borcard, D., Carvalho, G., Chirico, M., Caceres, M. D., Durand, S., … Weedon, J. (2022). *vegan: Community Ecology Package*. https://CRAN.R-project.org/package=vegan

Olm, M. R., Brown, C. T., Brooks, B., & Banfield, J. F. (2017). dRep: A tool for fast and accurate genomic comparisons that enables improved genome recovery from metagenomes through de-replication. *The ISME Journal*, *11*(12), 2864–2868. https://doi.org/10.1038/ismej.2017.126

857 Oni, F. E., Geudens, N., Omoboye, O. O., Bertier, L., Hua, H. G. K., Adiobo, A., Sinnaeve, D., Martins, J.
858 C., & Höfte, M. (2019). Fluorescent Pseudomonas and cyclic lipopeptide diversity in the
859 rhizosphere of cocoyam (Xanthosoma sagittifolium). *Environmental Microbiology*, *21*(3),
860 1019–1034. https://doi.org/10.1111/1462-2920.14520
861 Ordon, J., Thouin, J., Nakano, R. T., Ma, K.-W., Zhang, P., Huettel, B., Garrido-Oter, R., & Schulze-
862 Lefert, P. (2024). Chromosomal barcodes for simultaneous tracking of near-isogenic bacterial
863 strains in plant microbiota. *Nature Microbiology*, 1–13. https://doi.org/10.1038/s41564-024-
864 01619-8
865 Pacheco-Moreno, A., Stefanato, F. L., Ford, J. J., Trippel, C., Uszkoreit, S., Ferrafiat, L., Grenga, L.,
866 Dickens, R., Kelly, N., Kingdon, A. D. H., Ambrosetti, L., Nepogodiev, S. A., Findlay, K. C.,
867 Cheema, J., Trick, M., Chandra, G., Tomalin, G., Malone, J. G., & Truman, A. W. (2021). Pan-
868 genome analysis identifies intersecting roles for pseudomonas specialized metabolites in
869 potato pathogen inhibition. *eLife*, *10*, 1–46. https://doi.org/10.7554/eLife.71900
870 Parks, D. H., Chuvochina, M., Chaumeil, P.-A., Rinke, C., Mussig, A. J., & Hugenholtz, P. (2020). A
871 complete domain-to-species taxonomy for Bacteria and Archaea. *Nature Biotechnology*,
872 *38*(9), 1079–1086. https://doi.org/10.1038/s41587-020-0501-8
873 Parks, D. H., Imelfort, M., Skennerton, C. T., Hugenholtz, P., & Tyson, G. W. (2015). CheckM:
874 Assessing the quality of microbial genomes recovered from isolates, single cells, and
875 metagenomes. *Genome Research*, *25*(7), 1043–1055. https://doi.org/10.1101/gr.186072.114
876 Pervaiz, Z. H., Contreras, J., Hupp, B. M., Lindenberger, J. H., Chen, D., Zhang, Q., Wang, C., Twigg, P.,
877 & Saleem, M. (2020). Root microbiome changes with root branching order and root
878 chemistry in peach rhizosphere soil. *Rhizosphere*, *16*(June), 100249.
879 https://doi.org/10.1016/j.rhisph.2020.100249
880 Qiu, Z., Verma, J. P., Liu, H., Wang, J., Batista, B. D., Kaur, S., de Araujo Pereira, A. P., Macdonald, C.
881 A., Trivedi, P., Weaver, T., Conaty, W. C., Tissue, D. T., & Singh, B. K. (2022). Response of the
882 plant core microbiome to Fusarium oxysporum infection and identification of the
883 pathobiome. *Environmental Microbiology*, *24*(10), 4652–4669.
884 https://doi.org/10.1111/1462-2920.16194
885 Ren, X.-B., Dang, Y.-R., Liu, S.-S., Huang, K.-X., Qin, Q.-L., Chen, X.-L., Zhang, Y.-Z., Wang, Y.-J., & Li, P.-
886 Y. (2022). Identification and Characterization of Three Chitinases with Potential in Direct
887 Conversion of Crystalline Chitin into N,N′-diacetylchitobiose. *Marine Drugs*, *20*(3), 165.
888 https://doi.org/10.3390/md20030165
889 Saleem, M., Law, A. D., Sahib, M. R., Pervaiz, Z. H., & Zhang, Q. (2018). Impact of root system
890 architecture on rhizosphere and root microbiome. *Rhizosphere*, *6*(March), 47–51.
891 https://doi.org/10.1016/j.rhisph.2018.02.003
892 Sasse, J., Martinoia, E., & Northen, T. (2018). Feed Your Friends: Do Plant Exudates Shape the Root
893 Microbiome? *Trends in Plant Science*, *23*(1), 25–41.
894 https://doi.org/10.1016/j.tplants.2017.09.003
895 Scales, N. C., Huynh, K. T., Weihe, C., & Martiny, J. B. H. (2023). Desiccation induces varied responses
896 within a soil bacterial genus. *Environmental Microbiology*, *25*(12), 3075–3086.
897 https://doi.org/10.1111/1462-2920.16494
898 Seemann, T. (2014). Prokka: Rapid prokaryotic genome annotation. *Bioinformatics*, *30*(14), 2068–
899 2069. https://doi.org/10.1093/bioinformatics/btu153
900 Seethepalli, A., Dhakal, K., Griffiths, M., Guo, H., Freschet, G. T., & York, L. M. (2021). RhizoVision
901 Explorer: Open-source software for root image analysis and measurement standardization.
902 *AoB PLANTS*, *13*(6), plab056. https://doi.org/10.1093/aobpla/plab056
903 Shaiber, A., Willis, A. D., Delmont, T. O., Roux, S., Chen, L.-X., Schmid, A. C., Yousef, M., Watson, A.
904 R., Lolans, K., Esen, Ö. C., Lee, S. T. M., Downey, N., Morrison, H. G., Dewhirst, F. E., Mark

Welch, J. L., & Eren, A. M. (2020). Functional and genetic markers of niche partitioning among enigmatic members of the human oral microbiome. *Genome Biology*, *21*(1), 292. https://doi.org/10.1186/s13059-020-02195-w

Shalev, O., Ashkenazy, H., Neumann, M., & Weigel, D. (2021). Commensal Pseudomonas protect Arabidopsis thaliana from a coexisting pathogen via multiple lineage-dependent mechanisms. *ISME Journal*, *November*, 1–10. https://doi.org/10.1038/s41396-021-01168-6

Sharifi-Tehrani, A., Zala, M., Natsch, A., Moënne-Loccoz, Y., & Défago, G. (1998). Biocontrol of soil-borne fungal plant diseases by 2,4-diacetylphloroglucinol-producing fluorescent pseudomonads with different restriction profiles of amplified 16S rDNA. *European Journal of Plant Pathology*, *104*(7), 631–643. https://doi.org/10.1023/A:1008672104562

Simonin, M., Dasilva, C., Terzi, V., Ngonkeu, E. L. M., DIouf, Di., Kane, A., Béna, G., & Moulin, L. (2020). Influence of plant genotype and soil on the wheat rhizosphere microbiome: Evidences for a core microbiome across eight African and European soils. *FEMS Microbiology Ecology*, *96*(6), 1–18. https://doi.org/10.1093/femsec/fiaa067

Sondo, M., Wonni, I., Koïta, K., Rimbault, I., Barro, M., Tollenaere, C., Moulin, L., & Klonowska, A. (2023). Diversity and plant growth promoting ability of rice root-associated bacteria in Burkina-Faso and cross-comparison with metabarcoding data. *PLOS ONE*, *18*(11), e0287084. https://doi.org/10.1371/journal.pone.0287084

Song, S., Morales Moreira, Z., Briggs, A. L., Zhang, X.-C., Diener, A. C., & Haney, C. H. (2023). PSKR1 balances the plant growth–defence trade-off in the rhizosphere microbiome. *Nature Plants*, *9*(12), Article 12. https://doi.org/10.1038/s41477-023-01539-1

Song, Y., Wilson, A. J., Zhang, X. C., Thoms, D., Sohrabi, R., Song, S., Geissmann, Q., Liu, Y., Walgren, L., He, S. Y., & Haney, C. H. (2021). FERONIA restricts Pseudomonas in the rhizosphere microbiome via regulation of reactive oxygen species. *Nature Plants*, *7*(5), 644–654. https://doi.org/10.1038/s41477-021-00914-0

Spor, A., Roucou, A., Mounier, A., Bru, D., Breuil, M.-C., Fort, F., Vile, D., Roumet, P., Philippot, L., & Violle, C. (2020). Domestication-driven changes in plant traits associated with changes in the assembly of the rhizosphere microbiota in tetraploid wheat. *Scientific Reports*, *10*(1), Article 1. https://doi.org/10.1038/s41598-020-69175-9

Stevens, B. M., Creed, T. B., Reardon, C. L., & Manter, D. K. (2023). Comparison of Oxford Nanopore Technologies and Illumina MiSeq sequencing with mock communities and agricultural soil. *Scientific Reports*, *13*(1), Article 1. https://doi.org/10.1038/s41598-023-36101-8

Takamatsu, K., Toyofuku, M., Okutani, F., Yamazaki, S., Nakayasu, M., Aoki, Y., Kobayashi, M., Ifuku, K., Yazaki, K., & Sugiyama, A. (2023). α-Tomatine gradient across artificial roots recreates the recruitment of tomato root-associated Sphingobium. *Plant Direct*, *7*(12), e550. https://doi.org/10.1002/pld3.550

Tatusov, R. L., Galperin, M. Y., Natale, D. A., & Koonin, E. V. (2000). The COG database: A tool for genome-scale analysis of protein functions and evolution. *Nucleic Acids Research*, *28*(1), 33–36.

Terlouw, B. R., Blin, K., Navarro-Muñoz, J. C., Avalon, N. E., Chevrette, M. G., Egbert, S., Lee, S., Meijer, D., Recchia, M. J. J., Reitz, Z. L., van Santen, J. A., Selem-Mojica, N., Tørring, T., Zaroubi, L., Alanjary, M., Aleti, G., Aguilar, C., Al-Salihi, S. A. A., Augustijn, H. E., … Medema, M. H. (2023). MIBiG 3.0: A community-driven effort to annotate experimentally validated biosynthetic gene clusters. *Nucleic Acids Research*, *51*(D1), D603–D610. https://doi.org/10.1093/nar/gkac1049

Thoms, D., Chen, M. Y., Liu, Y., Moreira, Z. M., Luo, Y., Song, S., Wang, N. R., & Haney, C. H. (2023). Innate immunity can distinguish beneficial from pathogenic rhizosphere microbiota. *bioRxiv*, 2023.01.07.523123. https://doi.org/10.1101/2023.01.07.523123

Ting, C. P., Funk, M. A., Halaby, S. L., Zhang, Z., Gonen, T., & van der Donk, W. A. (2019). Use of a scaffold peptide in the biosynthesis of amino acid–derived natural products. *Science*, *365*(6450), 280–284. https://doi.org/10.1126/science.aau6232

Ustick, L. J., Larkin, A. A., & Martiny, A. C. (2023). Global scale phylogeography of functional traits and microdiversity in Prochlorococcus. *The ISME Journal*, *17*(10), Article 10. https://doi.org/10.1038/s41396-023-01469-y

von Stein, O. D., Thies, W. G., & Hofmann, M. (1997). A high throughput screening for rarely transcribed differentially expressed genes. *Nucleic Acids Research*, *25*(13), 2598–2602. https://doi.org/10.1093/nar/25.13.2598

Wang, C., Yu, Q.-Y., Ji, N.-N., Zheng, Y., Taylor, J. W., Guo, L.-D., & Gao, C. (2023). Bacterial genome size and gene functional diversity negatively correlate with taxonomic diversity along a pH gradient. *Nature Communications*, *14*(1), Article 1. https://doi.org/10.1038/s41467-023-43297-w

Wang, N. R., Wiesmann, C. L., Melnyk, R. A., Hossain, S. S., Chi, M.-H., Martens, K., Craven, K., & Haney, C. H. (2022). Commensal Pseudomonas fluorescens Strains Protect Arabidopsis from Closely Related Pseudomonas Pathogens in a Colonization-Dependent Manner. *mBio*, *13*(1). https://doi.org/10.1128/mbio.02892-21

Watanabe, T., Kanai, R., Kawase, T., Tanabe, T., Mitsutomi, M., Sakuda, S., & Miyashita, K. (1999). Family 19 chitinases of Streptomyces species: Characterization and distributionThe GenBank accession numbers for the sequences determined in this work are AB031745–AB031757 inclusive. *Microbiology*, *145*(12), 3353–3363. https://doi.org/10.1099/00221287-145-12-3353

Weisburg, W. G., Barns, S. M., Pelletier, D. A., & Lane, D. J. (1991). 16S ribosomal DNA amplification for phylogenetic study. *Journal of Bacteriology*, *173*(2), 697–703.

Widmer, F., Seidler, R. J., Gillevet, P. M., Watrud, L. S., & Di Giovanni, G. D. (1998). A Highly Selective PCR Protocol for Detecting 16S rRNA Genes of the Genus Pseudomonas (Sensu Stricto) in Environmental Samples. *Applied and Environmental Microbiology*, *64*(7), 2545–2553.

Yang, K., Fu, R., Feng, H., Jiang, G., Finkel, O., Sun, T., Liu, M., Huang, B., Li, S., Wang, X., Yang, T., Wang, Y., Wang, S., Xu, Y., Shen, Q., Friman, V.-P., Jousset, A., & Wei, Z. (2023). RIN enhances plant disease resistance via root exudate-mediated assembly of disease-suppressive rhizosphere microbiota. *Molecular Plant*. https://doi.org/10.1016/j.molp.2023.08.004

Yang, T., Wei, Z., Friman, V., Xu, Y., Shen, Q., Kowalchuk, G. A., & Jousset, A. (2017). Resource availability modulates biodiversity-invasion relationships by altering competitive interactions. *Environmental Microbiology*, *19*(8), 2984–2991. https://doi.org/10.1111/1462-2920.13708

Zai, X., Luo, W., Bai, W., Li, Y., Xiao, X., Gao, X., Wang, E., Wei, G., & Chen, W. (2021). Effect of Root Diameter on the Selection and Network Interactions of Root-Associated Bacterial Microbiomes in Robinia pseudoacacia L. *Microbial Ecology*, *82*, 391–402. https://doi.org/10.1007/s00248-020-01678-4

Zhang, M., & Kong, X. (2022). How plants discern friends from foes. *Trends in Plant Science*, *27*(2), 107–109. https://doi.org/10.1016/j.tplants.2021.11.001

Zheng, Y., Wang, J., Zhang, X., Lei, L., Yu, R., Yao, M., Han, D., Zeng, Q., & Li, X. (2023). Core root-associated prokaryotic community and its relationship to host traits across wheat varieties. *Journal of Experimental Botany*, *74*(8), 2740–2753. https://doi.org/10.1093/jxb/erad066

999 Tables

ASV	Antifungal isolates within ASV	median number of reads in Sheriff	median number of reads in Heerup	Pval
S1E05	0/1	1.0	0.0	0.0472
S2B12_S2C03	1/2	3.0	0.0	0.0322
ASV67	n/a	1.0	0.0	0.0098
H3E07_S3A09	1/2	1.0	0.0	0.0398

1000 **Table 1A. Enriched ASVs in Heerup and Sheriff at T2, with notice of the isolates that were**
1001 **antifungal in the *in vitro* screen. P values were determined using the Mann-Whitney U-test. ASVs**
1002 **were omitted from composition tests if the ASV is not seen in at least 50% of the samples in one of**
1003 **the groups.**
1004

ASV	Antifungal isolates within ASV	median number of reads in Sheriff	median number of reads in Heerup	Pval
H1D09_H2B05_H2D02_S1A03_S2D10_S3C01_S3E11_S3F07_S3H10	6/9	14.0	6.0	0.0305
H3E07_S3A09	1/2	1.0	0.0	0.0036
H3H08	0/1	1.0	0.0	0.0079

1005 **Table 1B. Enriched ASVs in Heerup and Sheriff across T1 and T2, with notice of the isolates that**
1006 **were antifungal in the *in vitro* screen. P values were determined using the Mann-Whitney U-test.**
1007 **ASVs were omitted from composition tests if the ASV is not seen in at least 50% of the samples in**
1008 **one of the groups.**
1009

	Input	Sequence used to identify taxonomy	(C/A)SVs	Species	Strains
16S Sanger sequencing	373 isolates	900- 1270 bp of 16S rRNA gene	65	17	n/a
Long-read amplicon sequencing	19 rhizoplane samples	880-970 bp of 16S rRNA gene	70	n/a	n/a
Full genome sequencing	112 isolates	Full genome	n/a	21	48

1010 **Table 2. Counts of *Pseudomonas* found during each method used in the study, based on the**
1011 **various taxonomic levels and their definition based on percent identity across the sequence.**

1012

BGC family	Known BGC	Product Class	Enriched in	Adjusted p value

2428	3-thiaglutamate	RiPP-like	n/a	0.22
2549	Viscosin	NRPS	n/a	0.09
2653	Arthrofactin A, anikasin, lokisin, stechlisin B2	NRPS	n/a	0.84
3049	Pf-5 pyoverdine	NRPS	Sheriff	**0.0297**
3453	2,4-diacetylphloroglucinol	T3PKS	n/a	0.37
3764	Tabtoxin	blactam	n/a	0.36

1013 **Table 3. BGC families in the strain library that were identified as known products and the cultivar**
1014 **they were enriched in, if applicable. Significant differences in the abundance of the BGC family**
1015 **between cultivars was calculated using the two-sided Wilcoxon Rank Sum test with fdr-**
1016 **adjustment using the Benjamini & Hochberg method.**

1017

1018 Figure Legends

1019 **Methods Figure 1. Sampling for Pseudomonas isolation, long-read 16S rRNA amplicon sequencing,**
1020 **and root scanning occurred along different root axis as well as across different time points.**
1021 **Created with Biorender.com.**

1022 **Figure 1. Composition of the Heerup and Sheriff *Pseudomonas* strain libraries identified by Sanger**
1023 **sequencing of minimum 900 bp of the 16S rRNA gene from 195 purified isolates from Heerup and**
1024 **178 purified isolates from Sheriff.** Each color represents a *Pseudomonas* species or CSV. A)
1025 Composition at the species level identified by sequence alignment to the NBCI 16S rRNA gene
1026 database. A legend identifying the top five most abundant species is shown. B) Composition at the
1027 CSV level, defined as 100% identity across a minimum of 900 bp of the 16S rRNA gene.

1028 **Figure S1. Rarefaction curve based on CSV identification during sampling of isolates.**

1029 **Figure 2. The percentage of the strain libraries which can inhibit the growth of *F. culmorum in vitro***
1030 **depended on cultivar of origin, but the ability to produce biosurfactants was not dependent on**
1031 **cultivar. P-values of Fisher's exact test are given above the bars. Strains *Serratia inhibens* S40 and**
1032 ***Pseudomonas fluorescens* SBW25 were used as the positive control for the antifungal assay and**
1033 **the biosurfactant assay, respectively.**

1034 **Supplemental Figure 2. Sequencing results from long-read 16S rRNA amplicon sequencing using**
1035 **Nanopore technology across 880-970 bp of the 16S rRNA gene.** A) Rarefaction plot for effective
1036 Shannon diversity and B) richness. C) Percent of reads per sample that were identified as
1037 *Pseudomonas*. D) Percent of *Pseudomonas* reads per sample that mapped to cultured isolates or
1038 uncultured sequences.

1039 **Figure 3. Pangenome of the 112 genomes.** A) Blue highlight represents an isolate cultured from
1040 Heerup, and an orange highlight represents an isolate cultured from Sheriff. Shaded bars indicate
1041 the presence of gene clusters in the genome. The core genome of 2,322 gene clusters is collapsed
1042 for increased clarity. A phylogenetic tree and key metadata including species/strain identification
1043 and phenotypic assay result is indicated. B) Highlight boxes and arrows indicates the missing gene
1044 cluster locus in the Heerup-isolated strains of *P. brassicacearum* strain R, and the missing three gene
1045 cluster loci in Sheriff-isolated strains, despite its presence in closely related (same species and strain)

1046 isolates. C) Highlight box and arrow indicates the missing one gene cluster locus in Sheriff-isolated
1047 strains of *P. simiae* despite its presence in closely related (same species) isolates.

1048 **Figure 4. Differences in biosynthetic potential between the Heerup and Sheriff strain libraries.** A)
1049 Number of BGCs per genome in isolates cultured from Heerup or Sheriff cultivar is not different
1050 (two-sided Wilcoxon Rank Sum test). The average number of BGCs per genome in Heerup and Sheriff
1051 is 11.98 with a standard deviation of ±2.22 and 11.53 with a standard deviation of ±1.55,
1052 respectively. B) Differentially abundant BGC families found in Heerup- or Sheriff-associated
1053 pseudomonads were calculated using the two-sided Wilcoxon Rank Sum test and multiple testing
1054 was accounted for using the Benjamini & Hochberg method. BGC families are color-coded along the
1055 x-axis by their predicted product class. X-axis highlight box indicates if the BGC family is enriched in
1056 Heerup (blue) or Sheriff (orange).

1057 **Figure 5. Distribution of BGCs in the species found in the *Pseudomonas* strain library. X-axis**
1058 **highlight box represents if the species is found only in Heerup (blue) or Sheriff (orange).** A)
1059 Number of BGCs per genome. True data points are overlaid the violin plot as filled circles. Significant
1060 differences in average BGCs per genome of a species between cultivars was calculated using the
1061 two-sided Wilcoxon Rank Sum test for the species *P. brassicacearum*, *P. siliginis*, and *P.*
1062 *asgharzadehiana,* and only $p < 0.05$ are displayed. B) Proportion of isolates of each species harboring
1063 the BGC family that is differentially enriched between Heerup and Sheriff. The Y-axis highlight box
1064 represents if the BGC family is enriched in Heerup (blue) or Sheriff (orange).

1065 **Figure 6. Root scanning was performed on four-week old plants to measure root morphology**
1066 **parameters.** A) Root system composition of Heerup and Sheriff divided into six root diameter
1067 ranges. The box plots display the median, the two hinges (25th and 75th percentile), and the upper
1068 and lower whiskers (extending to the largest and smallest values no further than 1.5 times the
1069 interquartile range). True data points are overlaid the boxplot as filled circles. P values derived from
1070 the two-sided Student T test are shown. B) Representative images of washed Heerup and Sheriff
1071 root systems after four weeks of growth.

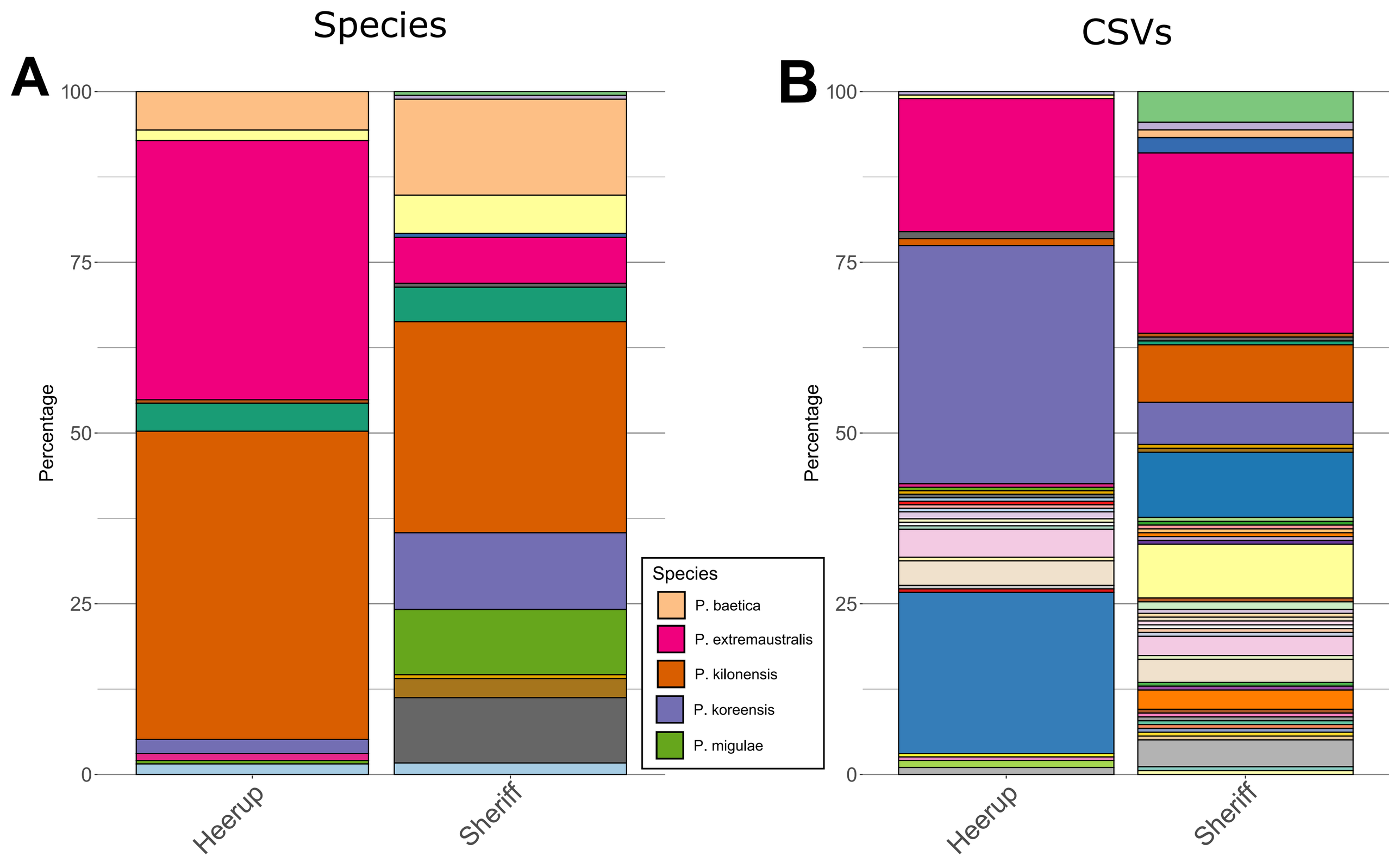
Species
A
100
75
50
25
0
Percentage
Heerup
Sheriff
Species
P. baetica
P. extremaustralis
P. kilonensis
P. koreensis
P. migulae
CSVs
B
100
75
50
25
0
Percentage
Heerup
Sheriff

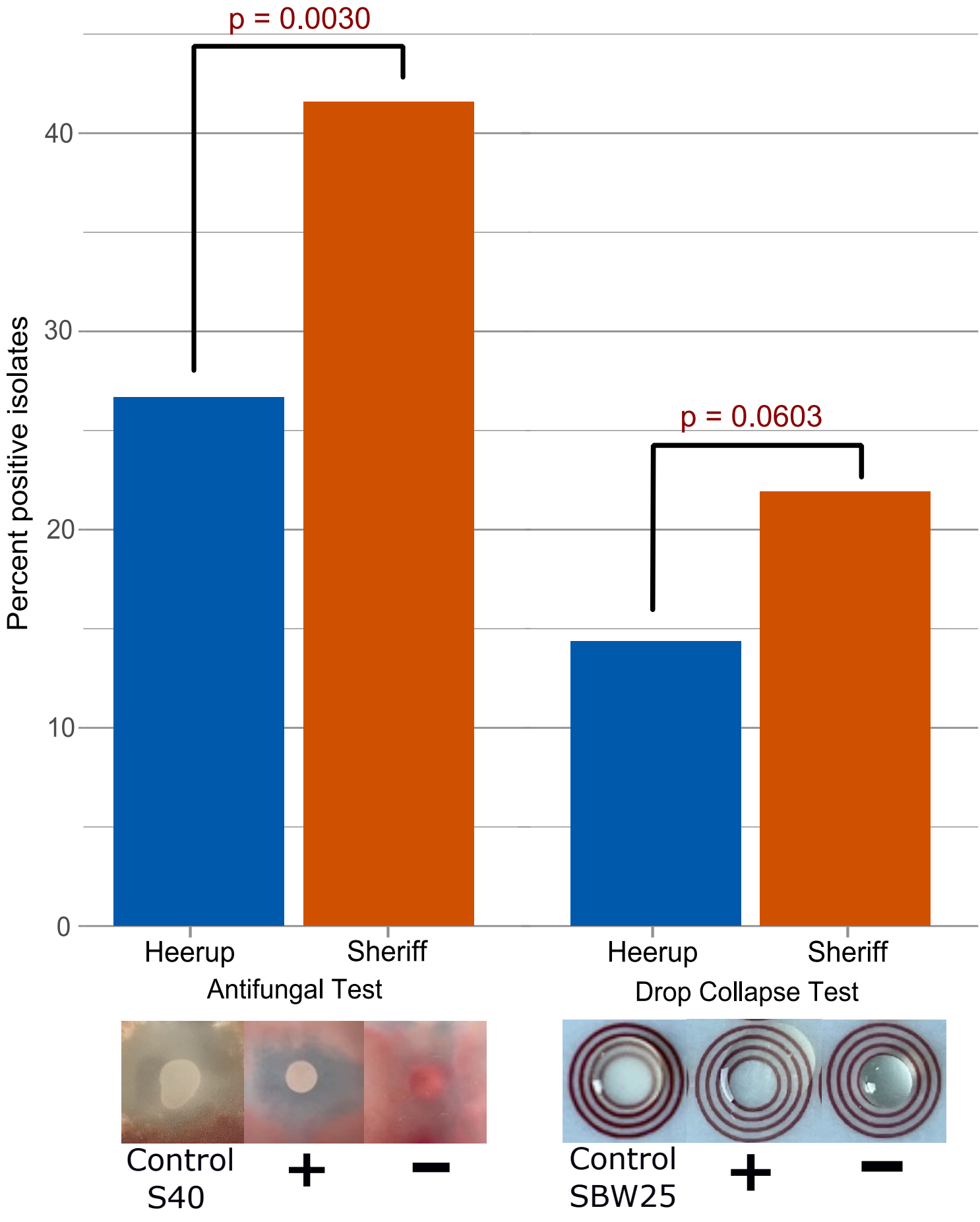
p = 0.0030
p = 0.0603
Percent positive isolates
0
10
20
30
40
Heerup
Sheriff
Antifungal Test
Heerup
Sheriff
Drop Collapse Test
Control
S40
+
−
Control
SBW25
+
−

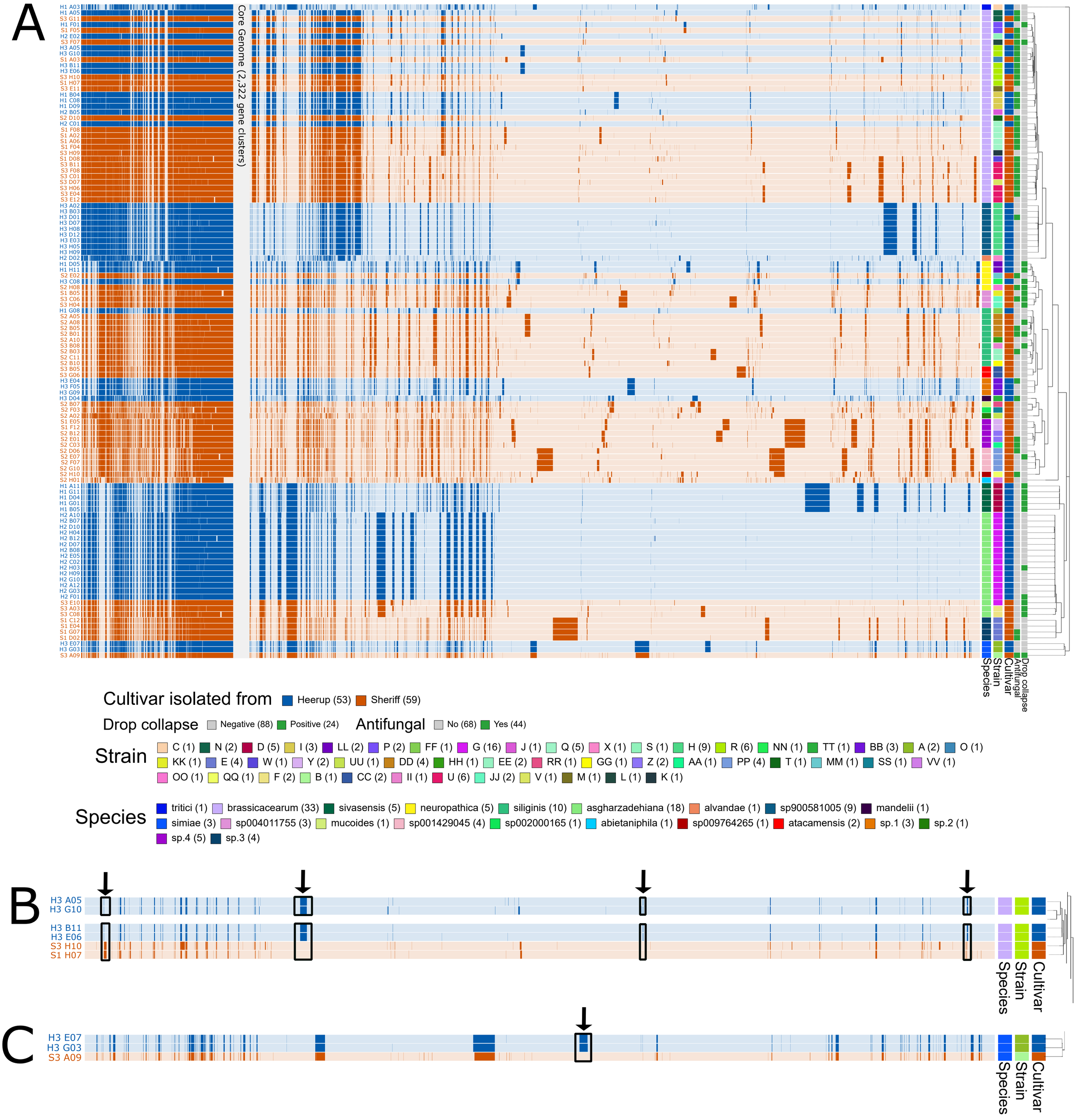
A
Core Genome (2,322 gene clusters)
Species
Strain
Cultivar
Antifungal
Drop collapse
Cultivar isolated from Heerup (53) Sheriff (59)
Drop collapse Negative (88) Positive (24)
Antifungal No (68) Yes (44)
Strain
C (1) N (2) D (5) I (3) LL (2) P (2) FF (1) G (16) J (1) Q (5) X (1) S (1) H (9) R (6) NN (1) TT (1) BB (3) A (2) O (1)
KK (1) E (4) W (1) Y (2) UU (1) DD (4) HH (1) EE (2) RR (1) GG (1) Z (2) AA (1) PP (4) T (1) MM (1) SS (1) VV (1)
OO (1) QQ (1) F (2) B (1) CC (2) II (1) U (6) JJ (2) V (1) M (1) L (1) K (1)
Species
tritici (1) brassicacearum (33) sivasensis (5) neuropathica (5) siliginis (10) asgharzadehiana (18) alvandae (1) sp900581005 (9) mandelii (1)
simiae (3) sp004011755 (3) mucoides (1) sp001429045 (4) sp002000165 (1) abietaniphila (1) sp009764265 (1) atacamensis (2) sp.1 (3) sp.2 (1)
sp.4 (5) sp.3 (4)
B
H3 A05
H3 G10
H3 B11
H3 E06
S3 H10
S1 H07
Species
Strain
Cultivar
C
H3 E07
H3 G03
S3 A09
Species
Strain
Cultivar

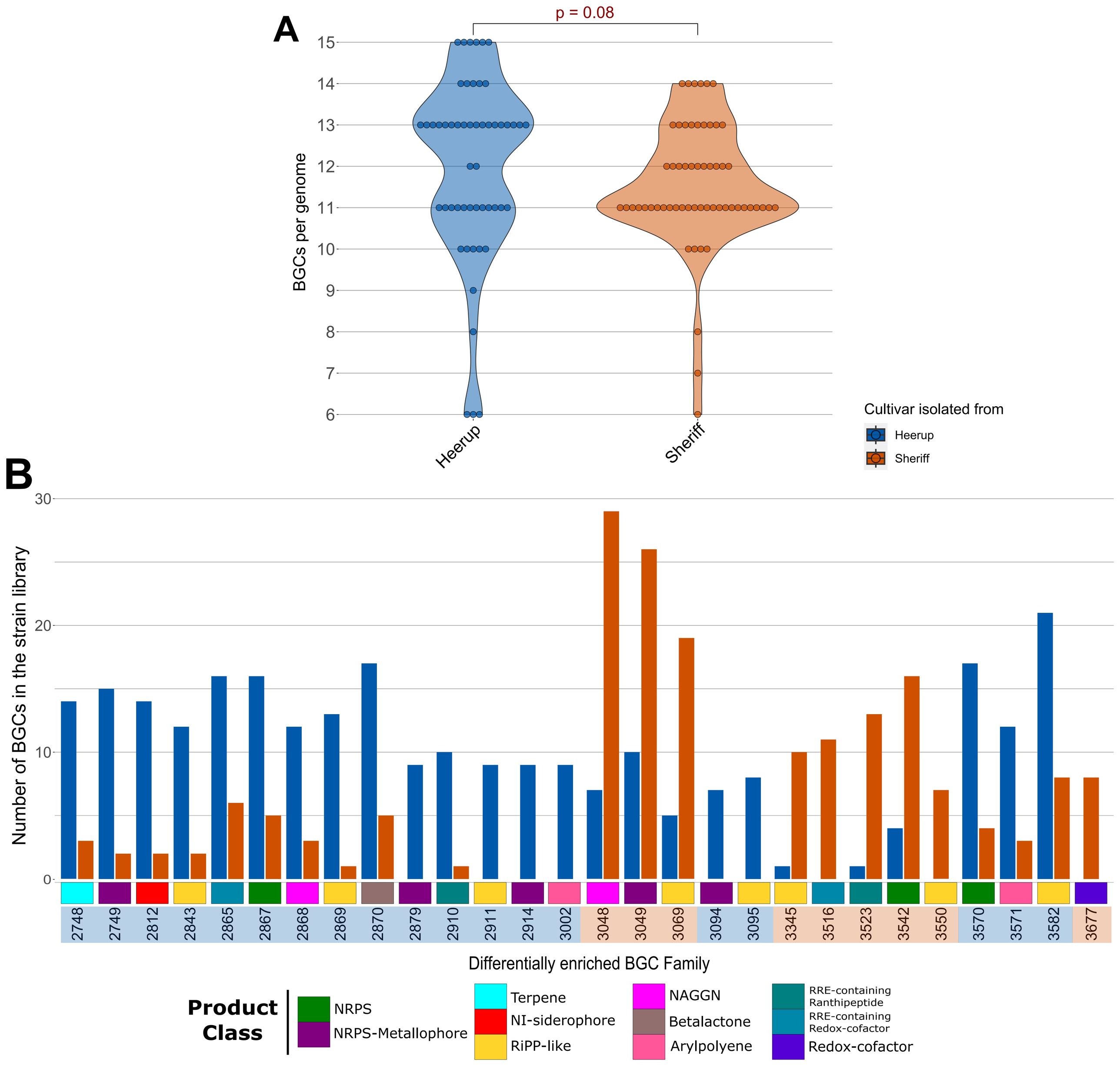
A
p = 0.08
BGCs per genome
15
14
13
12
11
10
9
8
7
6
Heerup
Sheriff
Cultivar isolated from
Heerup
Sheriff
B
Number of BGCs in the strain library
30
20
10
0
2748
2749
2812
2843
2865
2867
2868
2869
2870
2879
2910
2911
2914
3002
3048
3049
3069
3094
3095
3345
3516
3523
3542
3550
3570
3571
3582
3677
Differentially enriched BGC Family
Product Class
NRPS
NRPS-Metallophore
Terpene
NI-siderophore
RiPP-like
NAGGN
Betalactone
Arylpolyene
RRE-containing Ranthipeptide
RRE-containing Redox-cofactor
Redox-cofactor

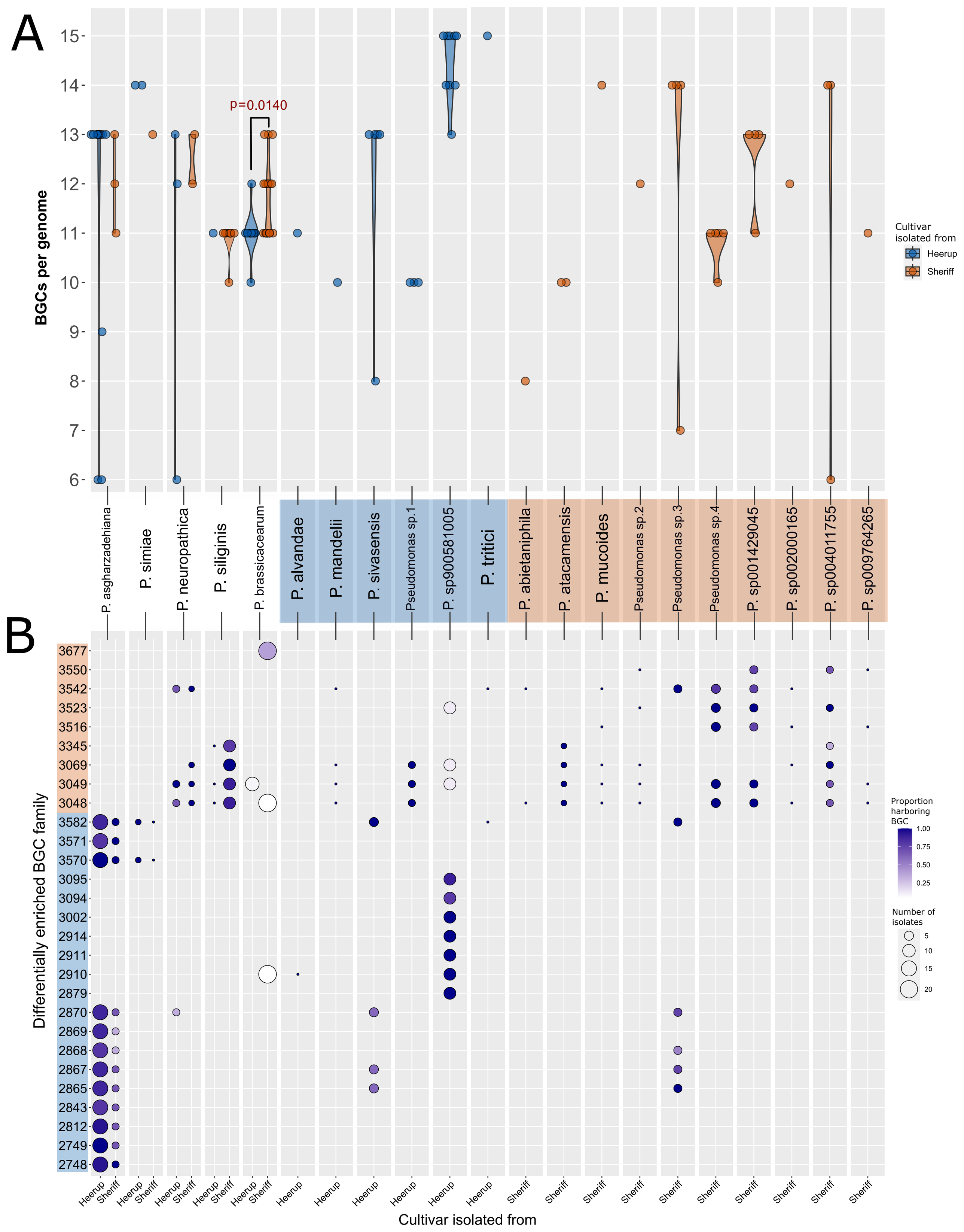
A
BGCs per genome
p=0.0140
Cultivar isolated from
Heerup
Sheriff
B
Differentially enriched BGC family
P. asgharzadehiana
P. simiae
P. neuropathica
P. siliginis
P. brassicacearum
P. alvandae
P. mandelii
P. sivasensis
Pseudomonas sp.1
P. sp900581005
P. tritici
P. abietaniphila
P. atacamensis
P. mucoides
Pseudomonas sp.2
Pseudomonas sp.3
Pseudomonas sp.4
P. sp001429045
P. sp002000165
P. sp004011755
P. sp009764265
Proportion harboring BGC
Number of isolates
Cultivar isolated from

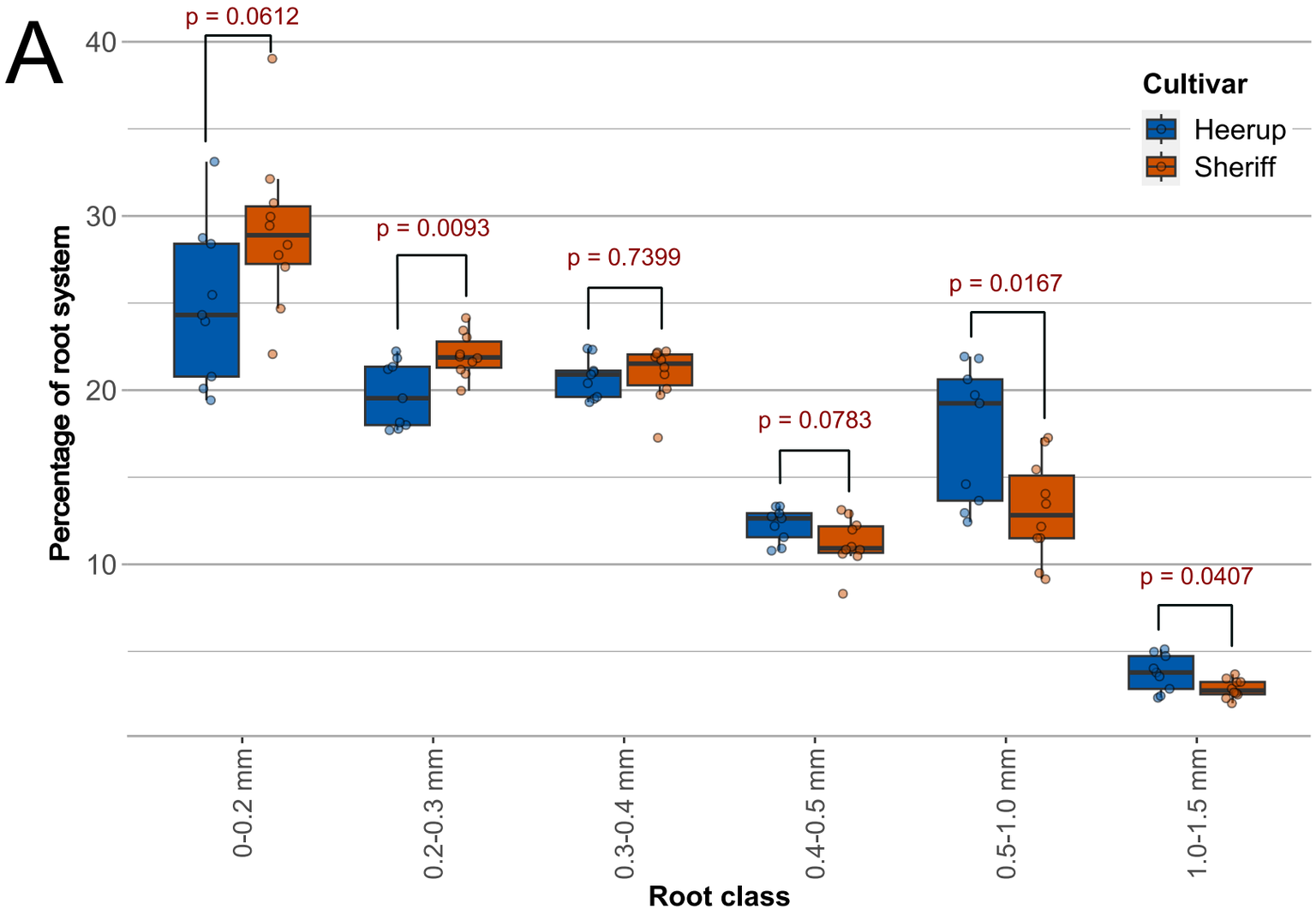
A
p = 0.0612
p = 0.0093
p = 0.7399
p = 0.0783
p = 0.0167
p = 0.0407
Cultivar
Heerup
Sheriff
Percentage of root system
40
30
20
10
0-0.2 mm
0.2-0.3 mm
0.3-0.4 mm
0.4-0.5 mm
0.5-1.0 mm
1.0-1.5 mm
Root class

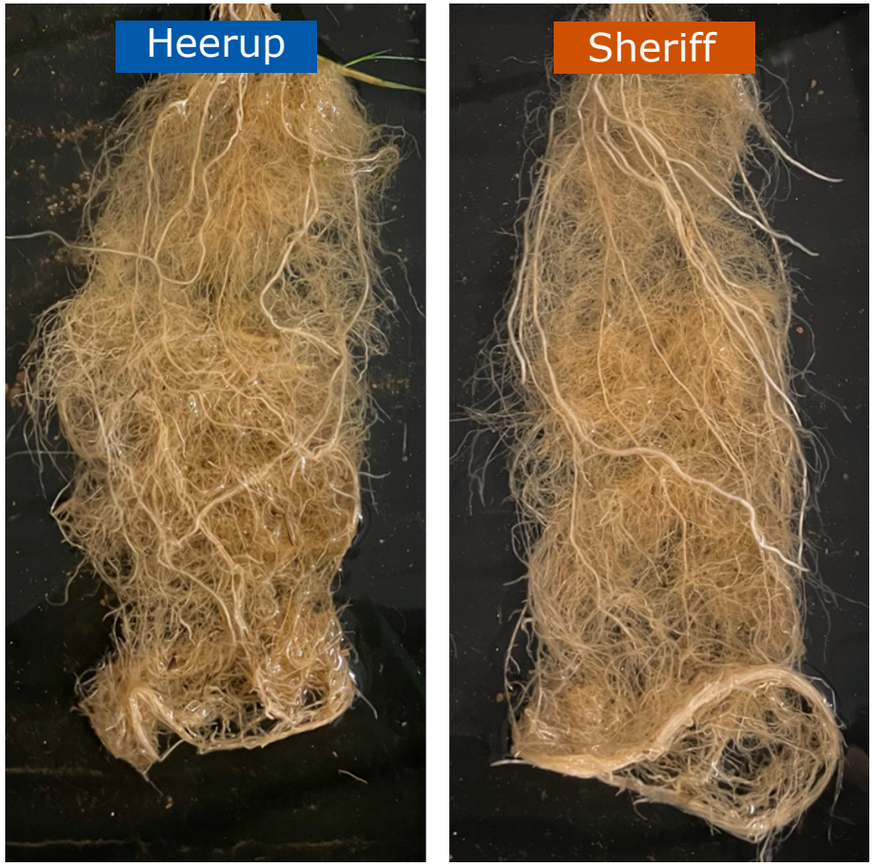
B
Heerup
Sheriff

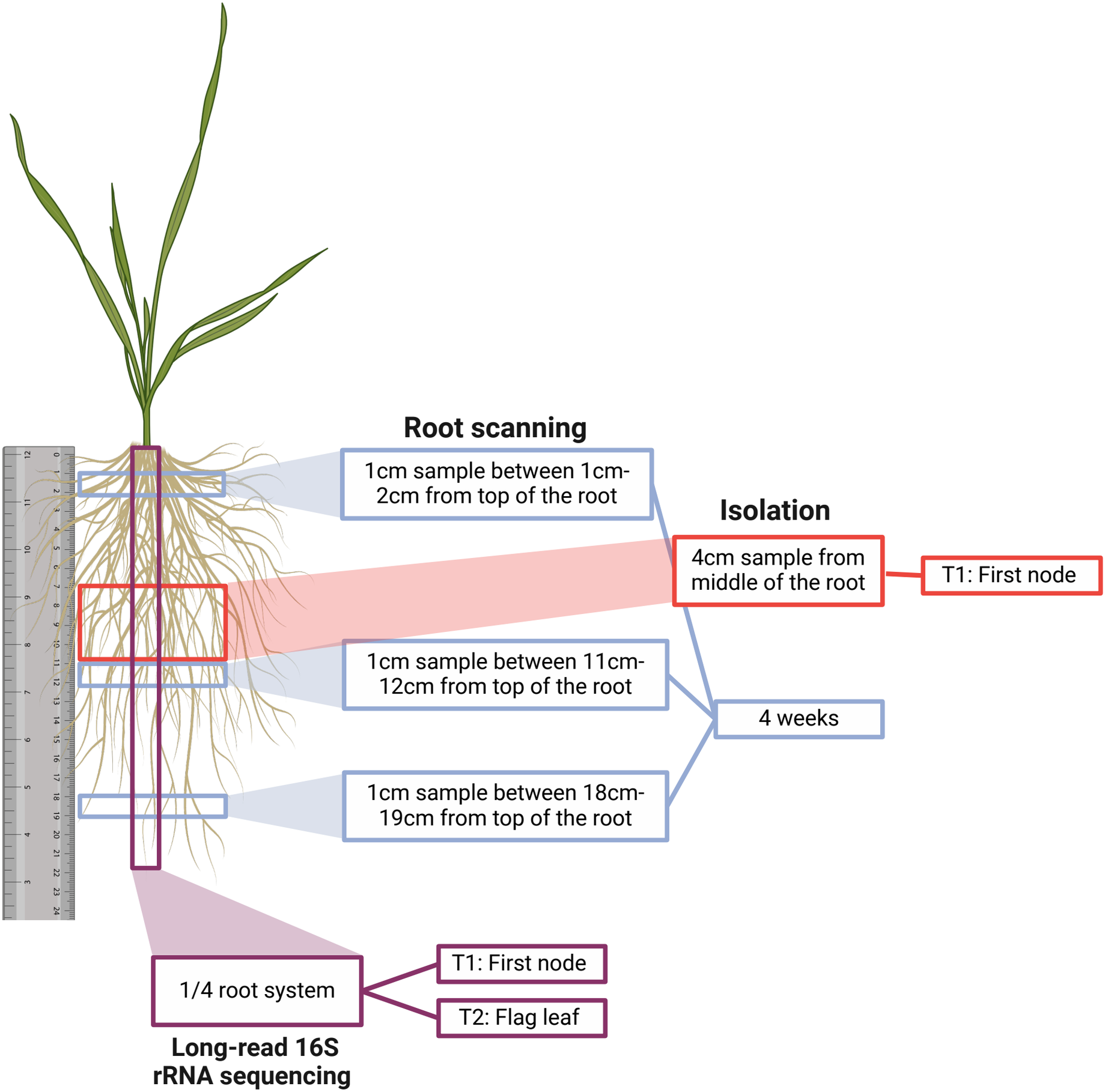
Root scanning
1cm sample between 1cm-2cm from top of the root
Isolation
4cm sample from middle of the root
T1: First node
1cm sample between 11cm-12cm from top of the root
4 weeks
1cm sample between 18cm-19cm from top of the root
1/4 root system
T1: First node
T2: Flag leaf
Long-read 16S rRNA sequencing